Outlier-Resistant Non-Fragile Control of Nonlinear Networked Systems Under DoS Attacks and Multi-Variable Event-Triggered SC Protocol

Jian Liu, *Member, IEEE*, Jiachen Ke, Jinliang Liu, *Member, IEEE*, Xiangpeng Xie, *Senior Member, IEEE*, and Engang Tian, *Member, IEEE*

***Abstract*— In this article, the outlier-resistant (OR) observer-based secure control problem is investigated for nonlinear networked systems under randomly activated denial-of-service (RADoS) attacks and stochastic communication (SC) protocol. In virtue of zero-order holder (ZOH) technique, an attack compensation scheme is adopted to alleviate the adverse effects brought by RADoS attacks. By introducing multiple internal dynamic variables (MIDVs), a novel multi-variable event-triggered stochastic communication (MVET-SC) protocol is put forward to enhance the design flexibility and prevent the occurrence of data conflicts. Moreover, the non-fragile fuzzy controller is applied due to the inaccuracies in practical applications. Comprehensively taking the above factors into account, the asymptotic stability of the augmented fuzzy system can be ensured under the presented sufficient criteria. Meanwhile, the parameters of the OR observer-based secure controller are derived according to the obtained design conditions. In the end, a simulation example of mass-spring-damping system (MSDS) demonstrates the validity of the non-fragile secure control approach with OR observer.**

***Index Terms*— Denial-of-service attacks, event-triggered mechanism, non-fragile secure control, outlier-resistant observer, stochastic communication protocol.**

I. Introduction

UNDER the integration of communication and computer technology, networked control systems (NCSs) have gained plentiful research interests due to the prospective applications in power systems [1], smart grids [2], mobile robots [3], etc [4], [5]. In NCSs, the interconnection between the open communication network and local physical components is susceptible to potential attackers, which may result in substantial threats to the focused system performance. As presented in existing literature, denial-of-service (DoS) attacks [6] and deception attacks [7], [8] are frequently investigated in the secure control/estimation problems. To mention a few, Gu et al. [9] designed a secure path tracking control strategy for autonomous ground vehicles. In [10], the attack-resilient filter issue has been addressed for interval type-2 (IT-2) fuzzy system in the presence of event-triggered (ET) communication mechanism and DoS attacks. The malicious behaviors of DoS attacks dedicate to block the transmitted signals in communication network and cause the deterioration on system performance. In real-word scenarios, a wealth of concerns has been focused on the security events, such as US Southwest blackout occurred in 2011 and Stuxnet malware incident [11]. Thus, it is considerably imperative to develop secure control scheme for NCSs against malignant DoS attacks.

In addition to the security issue, communication bandwidth constraint is another network-induced phenomenon. Under the requirement of confined network resources, the so-called event-triggered scheme (ETS) is adopted in [12], [13], and [14], which can determine whether the sampled information is transmitted via a communication channel according to the designed triggered condition. By virtue of this mechanism, the more efficient transmission processes are obtained in comparison with the traditional time-triggered approach. In the past few decades, plentiful ET mechanisms are emerged in regard to the limited communication resources. To name a few, Pan et al. [15] addressed a transmission delay-based ET control problem for IT-2 fuzzy networked systems. In [16], a memory-based ET strategy was presented for power systems by utilizing the previous released data. The authors in [17] investigated the secure controller design method for NCSs with hybrid-triggered mechanism and randomly activated cyber attacks. On account of the aforesaid observations, various ET control policies have been put forward to mitigate the network occupancy. In the meantime, a dynamic event-triggered scheme (DETS) [18], [19], [20] with internal dynamic variable (IDV) is paid extensive

Manuscript received 6 June 2023; revised 24 September 2023; accepted 15 December 2023. Date of publication 10 January 2024; date of current version 24 January 2024. This work was supported in part by the National Natural Science Foundation of China under Grant 62001210, Grant 62373252, Grant 61973152, and Grant 62373196; in part by the Natural Science Foundation of Jiangsu Province of China under Grant BK20211290; and in part by the Postgraduate Research and Practice Innovation Program of Jiangsu Province under Grant KYCX23_1887. The associate editor coordinating the review of this manuscript and approving it for publication was Dr. Abdallah Shami. *(Corresponding author: Jinliang Liu.)*

Jian Liu and Jiachen Ke are with the College of Information Engineering, Nanjing University of Finance and Economics, Nanjing 210023, China (e-mail: by.liujian@gmail.com; 2212602143@qq.com).

Jinliang Liu is with the School of Computer Science, Nanjing University of Information Science and Technology, Nanjing 210044, China (e-mail: liujinliang@vip.163.com).

Xiangpeng Xie is with the Institute of Advanced Technology, Nanjing University of Posts and Telecommunications, Nanjing 210023, China (e-mail: xiexiangpeng1953@163.com).

Engang Tian is with the School of Optical-Electrical and Computer Engineering, University of Shanghai for Science and Technology, Shanghai 200093, China (e-mail: tianengang@163.com).

Digital Object Identifier 10.1109/TIFS.2024.3352404

attention owing to the lower triggered rate. Nevertheless, a single IDV is utilized to regulate the triggered threshold in the current stage of research. It is worth mentioning that the large error and the abnormal state of IDV may occur in ET process due to the complicated external circumstance [21]. Hence, this article endeavors to combine the information of the latest triggered signal and multiple internal dynamic variables (MIDVs) such that the triggered condition no longer relies on a single IDV.

In the shared communication channel, the occurrence of signal congestion may lead to the fact that the useful information is rough to be obtained by physical components in NCSs, which will degrade the control performance. To overcome this adverse impact, communication protocols are exploited to schedule the transferred data on account of the corresponding selective standards. Generally, communication protocols can be outlined as stochastic communication (SC) protocol [22], [23], round-robin (RR) protocol [24], [25] and try-once-discard (TOD) protocol [26], [27]. Significantly, SC protocol has been applied in industrial implementation [28]. Its trait is concluded that all sensor nodes have a possibility to access the communication channel with a stochastic sequence. As an effective tactic of economizing network utilization, the topic of SC protocol has received constantly increasing research attention. For example, Wan et al. [29] investigated the quantization-based state estimation issue for genetic regulatory networks scheduling by SC protocol. In [30], a ϵ-stealthy optimal attack scheme has been proposed for cyber-physical systems under SC protocol. So far, it can be witnessed that the secure ET control problem for NCSs with SC protocol has not been fully addressed, which promote our current research.

From engineering perspective, the measurement output obtained by the observer in NCSs is vulnerable to the impacts of unpredictably exogenous environment, cyber attacks, sensor noises and so on. In recent literature [31], [32], it can be named as measurement outliers, which may cause the anomalous magnitude changes. If such a phenomenon is directly neglected, it is relatively possible that the controller/estimator will be inapplicable for attaining the desired performance. Therefore, the outlier-resistant (OR) control/estimator scheme for NCSs is worthy of significance. The measurement outliers-related topic has aroused the evident research interests and some theoretical results have been published. In [33], a set-membership filtering issue has been investigated by proposing an outlier detection method. In addition, Li et al. [34] designed a novel OR state estimation approach under the utilization of a saturation function. Based on the above-mentioned discussion, the secure fuzzy control issue subject to measurement outliers and DoS attacks has not been adequately resolved. This is another motivation in this article.

Illuminated by the aforesaid analysis, the OR observer-based secure ET control scheme will be devised for fuzzy networked systems against randomly activated denial-of-service (RADoS) attacks under SC protocol. In comparison with the existing results, the central features of this paper are outlined as follows:

1) The DETS in [35] can dynamically regulate the ET threshold, however, the complex disturbance may exist in the ET process and causes dramatic error. To obviate this obstacle, a novel multi-variable ET scheme (MVETS) is designed to integrate the measured signals at the current sampled times and the previous ET times. Meanwhile, MIDVs are utilized in MVETS by introducing a group of weight coefficients such that the design flexibility can be effectively improved in comparison with [35].
2) On the basis of zero-order holder (ZOH) technique, an attack compensation approach is utilized to lessen the negative impacts led by RADoS attacks. Furthermore, the phenomenon of gain variation in engineering practice is involved in the controller design. Compared with the control scheme in [21], the OR observer-based non-fragile control mechanism in this article can appropriately tackle the measurement outliers.
3) In order to decrease the possibility of data conflicts in communication channel, a multi-variable ET SC (MVET-SC) protocol is put forward to schedule the transmitted signal when the ET condition is satisfied. Different from [35] and [36], MVET-SC protocol is mainly based on the randomness of node selection, and a Markov chain with known transition probability is applied. On account of MVET-SC protocol, we construct a new Lyapunov function to reflect the behaviors of MIDVs and SC protocol scheduling.

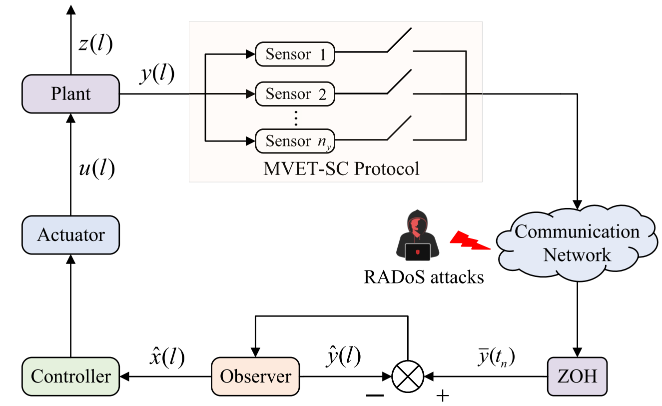

Fig. 1. The diagram of NCSs under RADoS attacks and MVET-SC protocol.

The remaining arrangements of this work can be presented as follows. Section II describes the details of MVET-SC protocol, RADoS attacks and OR observer-based control policy. In Section III, the major analysis results are elaborated. Section IV validates the feasibility of the proposed control scheme by a simulation example. Ultimately, Section V summarizes this paper.

Notations: $sym\{\mathcal{K}\}$ denotes the sum of $\mathcal{K}$ and $\mathcal{K}^T$. $\mathcal{K}_N$ stands for the $1 \times N$ vector $[\mathcal{K}, \cdots, \mathcal{K}]$. 0_{N-1}^N represents the matrix $[0_{N-1}^T, \cdots, 0_{N-1}^T]^T$. Other mathematical symbols utilized in this article are normal.

II. Problem Formulation

The nonlinear NCSs with MVET-SC protocol subject to RADoS attacks are depicted in Fig. 1. Then, the characteristics of RADoS attacks and MVET-SC protocol will be precisely expounded in this section.

A. The IT-2 Fuzzy System

An IT-2 fuzzy dynamics with m rules is applied to describe nonlinear networked systems and the p-th rule can be presented as follows.

RULE p: **IF** $\varsigma_1(x(l))$**is**$\mathcal{W}_1^p$, $\varsigma_2(x(l))$**is**$\mathcal{W}_2^p$, $\cdots$, $\varsigma_q(x(l))$**is**$\mathcal{W}_q^p$, **THEN**

$$\begin{cases} x(l+1) = A_p x(l) + B_p u(l) + B_{wp} w(l) \\ y(l) = C_{1p} x(l) \\ z(l) = C_{2p} x(l) \end{cases} \tag{1}$$

where $\mathcal{W}_i^p$ ($i = 1, 2, \cdots, q$ and $p = 1, 2, \cdots, m$) denotes the fuzzy sets corresponding to the premise variable $\varsigma_i(x(l))$. The positive scalars q and m are the quantity of the fuzzy sets and the IF-THEN rules. $x(l) \in \mathbb{R}^{n_x}$, $y(l) \in \mathbb{R}^{n_y}$, $z(l) \in \mathbb{R}^{n_z}$, $u(l) \in \mathbb{R}^{n_u}$, $w(l) \in \mathcal{L}_2[0, \infty)$ stand for the system state, the measured signal, the control output vector, the control input vector and the external interference, respectively. A_p, B_p, B_{wp}, C_{1p}, C_{2p} represent the given coefficient matrices with compatible dimensions. The p-th firing strength in accordance with the p-th rule is defined in the following format:

$$\tilde{\chi}_p(x(l)) = [\underline{\chi}_p(x(l)), \overline{\chi}_p(x(l))] \tag{2}$$

where

$$\underline{\chi}_p(x(l)) = \prod_{i=1}^{q} \underline{\upsilon}_{\mathcal{W}_i^p}(\varsigma_i(x(l))), \quad \overline{\chi}_p(x(l)) = \prod_{i=1}^{q} \overline{\upsilon}_{\mathcal{W}_i^p}(\varsigma_i(x(l))).$$

$\underline{\upsilon}_{\mathcal{W}_i^p}(\varsigma_i(x(l)))$ and $\overline{\upsilon}_{\mathcal{W}_i^p}(\varsigma_i(x(l)))$ represent the lower and upper membership functions (LUMFs) with $\overline{\upsilon}_{\mathcal{W}_i^p}(\varsigma_i(x(l))) \geq \underline{\upsilon}_{\mathcal{W}_i^p}(\varsigma_i(x(l))) \geq 0$. $\underline{\chi}_p(x(l))$ and $\overline{\chi}_p(x(l))$ are the lower and upper grades with $\overline{\chi}_p(x(l)) \geq \underline{\chi}_p(x(l)) \geq 0$. Based on the aforementioned content, the IT-2 fuzzy system (1) is presented as

$$\begin{cases} x(l+1) = \sum_{p=1}^{m} \mu_p(x(l))[A_p x(l) + B_p u(l) + B_{wp} w(l)] \\ y(l) = \sum_{p=1}^{m} \mu_p(x(l)) C_{1p} x(l) \\ z(l) = \sum_{p=1}^{m} \mu_p(x(l)) C_{2p} x(l) \end{cases} \tag{3}$$

where $\mu_p(x(l)) = \hat{\mu}_p(x(l)) / \sum_{p=1}^{m} \hat{\mu}_p(x(l))$, $\hat{\mu}_p(x(l)) = \underline{\alpha}_p(x(l))\underline{\chi}_p(x(l)) + \overline{\alpha}_p(x(l))\overline{\chi}_p(x(l))$. $\mu_p(x(l))$ denotes the normalized membership with $\sum_{p=1}^{m} \mu_p(x(l)) = 1$. The nonlinear weighting functions $\underline{\alpha}_p(x(l)) \in [0, 1]$ and $\overline{\alpha}_p(x(l)) \in [0, 1]$ satisfy $\underline{\alpha}_p(x(l)) + \overline{\alpha}_p(x(l)) = 1$.

B. The MVET-SC Protocol

In an effor to alleviate the communication bandwidth pressure, a DETS with IDV is exploited to decrease the transmission of unnecessary data packets. According to [35], it can be conventionally constructed in the following form:

$$t_{n+1} = \min_{l \in \mathbb{N}^+} \{l > t_n | \frac{1}{a}\lambda(l) + \mu y^T(l) y(l) \leq e_M^T(l) e_M(l)\} \tag{4}$$

where t_n ($n = 0, 1, 2, \cdots$) is the ET time instant and the initial value $t_0 \geq 0$. $e_M(l) = y(l) - y(t_n)$ stands for the error of the measured output at the current sampled time instant and the previous triggered time instant. $a > 0$ and $\mu \in (0, 1)$ are the given parameters. $\lambda(l)$ denotes the IDV with the iteration $\lambda(l+1) = \kappa\lambda(l) - e_M^T(l) e_M(l) + \mu y^T(l) y(l)$.

Once the condition (4) is gratified, the current sampled data will be released to the communication network. Meanwhile, the IDV can dynamically adjust the ET criterion according to the predetermined iteration. Under the motivation of this strategy, we aim to propose a novel DETS with MIDVs, which make the dynamic adjustment process more flexible. To achieve this purpose, a set of weight coefficients will be applied to connect MIDVs. Then, the MVETS is designed as follows:

$$\begin{cases} t_{n+1} = \min_{l \in \mathbb{N}^+} \{l > t_n | \sum_{j=1}^{N} \frac{\theta_j}{a_j} \lambda_j(l) - \Xi(l) < 0\} \\ \Xi(l) = e_M^T(l) \Theta e_M(l) - \varepsilon_M^1 y^T(l) \Theta y(l) - \varepsilon_M^2 y^T(t_n) \Theta y(t_n) \\ \lambda_j(l+1) = \kappa_j \lambda_j(l) - \theta_j \Xi(l), \quad j = 1, 2, \cdots, N \end{cases} \tag{5}$$

where $\lambda_j(l)$ are the MIDVs with the initialization $\lambda_j(0) \geq 0$. N symbolizes the maximum number of the MIDVs. Θ is the positive-definite weight matrix to be determined. $\theta_j > 0$ stands for the given weight coefficient with $\sum_{j=1}^{N} \theta_j = 1$. $a_j > 0$, $\varepsilon_M^1 \in (0, 1)$, $\varepsilon_M^2 \in (0, 1)$, $\kappa_j \in (0, 1)$ are the prescribed MVETS parameters with $\varepsilon_M^1 + \varepsilon_M^2 < 1$ and $\kappa_j > \kappa_{min} \triangleq \sum_{j=1}^{N} \frac{\theta_j^2}{a_j}$.

Remark 1: In comparison with the existing DETS in [35], the proposed MVETS can effectively improve the design flexibility and preferably reflect the ET dynamicity by introducing MIDVs $\lambda_j(l)$ and the weight matrix Θ. On the other hand, the utilization of MIDVs $\lambda_j(l)$ is also related to the dramatic error in the ET process. To be specific, when the complicated environment abruptly changes, the measured signal $y(l)$ is vulnerable to a variety of factors, such as unknown exogenous disturbance, sensor failures and so on. Thus, these factors may result in the abnormal magnitude of $y(l)$ such that the large error $e_M(l)$ occurs in the ET condition (4). It is apparent that the DETS proposed in [35] not takes this aspect into account. For the applied MVETS (5), the iteration of MIDVs is not only related to the current measurement signal $y(l)$, but also to the value $y(t_n)$. Meanwhile, they are properly combined by the parameters ε_M^1 and ε_M^2. Additionally, the ET threshold in MVETS is collectively adjusted by MIDVs rather than a single IDV, which has been presented in the aforementioned DETS [35]. Based on the above description, the dramatic error appeared in ET process can be reduced under the designed MVETS.

Remark 2: According to (5), the current sampled signal $y(l)$ and the latest ET signal $y(t_n)$ are combined to determine whether the triggered condition is met. In the proposed MVETS, a buffer is adopted to record the triggered data $y(t_n)$. Evidently, the sequence $\{t_n\}_{n=0}^{+\infty}$ is a subset of time sequence. Under such a mechanism, the term $y(t_n)$ in (5) will not be null at each time instant l. When judging the ET condition, the recorded ET data $y(t_n)$ and the current sampled signal $y(l)$ can be employed to calculate the error $e_M(l)$. On the other hand, when the parameters $\varepsilon_M^2 \to 0$, $\Theta = I$ and $N = 1$, the MVETS recovers the DETS in [35]. Thus, it is apparently concluded that the designed MVETS is more general. For the convenience of analysis, the condition $l \in [t_n, t_{n+1})$ will be omitted to demonstrate in the subsequent sections.

Under the restricted communication resources, the attention needs to be focused on decreasing the incidence of data collisions. In the consideration of the communication network between the sensors and the observer-based controller, the released measured output $y(t_n) = [y_1^T(t_n), y_2^T(t_n), \cdots, y_{n_y}^T(t_n)]^T$ can be scheduled by SC protocol when the MVETS condition (5) is gratified. In this paper, SC protocol is employed to randomly select the transmitted sensor node $\delta_{t_n} \in \mathbb{Q} \triangleq \{1, 2, \cdots, n_y\}$ in the light of a Markov chain [28], where the transition probabilities are described as

$$\zeta_{ts} = Prob\{\delta_{t_{n+1}} = s | \delta_{t_n} = t\} \tag{6}$$

where $\zeta_{ts} \in [0, 1]$ $(t, s \in \mathbb{Q})$ and $\sum_{s=1}^{n_y} \zeta_{ts} = 1$.

By denoting $\bar{y}(t_n) = [\bar{y}_1^T(t_n), \bar{y}_2^T(t_n), \cdots, \bar{y}_{n_y}^T(t_n)]^T$ as the measurement signal to the observer, an updating law for the $\hbar$-th measured signal $\bar{y}_\hbar(t_n)$ $(\hbar \in \mathbb{Q})$ can be obtained by

$$\bar{y}_\hbar(t_n) = \begin{cases} y_\hbar(t_n), & \text{if } \hbar = \delta_{t_n} \\ \bar{y}_\hbar(t_{n-1}), & \text{otherwise.} \end{cases} \tag{7}$$

In an effort to facilitate the next analysis, a Kronecker delta function $\varphi(\tilde{m} - \tilde{n}) \in \{0, 1\}$ is adopted. When $\tilde{m} = \tilde{n}$, $\varphi(\tilde{m} - \tilde{n}) = 1$. Otherwise, $\varphi(\tilde{m} - \tilde{n}) = 0$. With the assistance of Kronecker delta function $\varphi(\cdot)$, the following formula can be readily deduced:

$$\bar{y}(t_n) = \Phi_{\delta_{t_n}} y(t_n) + \bar{\Phi}_{\delta_{t_n}} \bar{y}(t_{n-1}) \tag{8}$$

where the updating matrix $\Phi_{\delta_{t_n}} = \text{diag}\{\varphi(\delta_{t_n} - 1), \varphi(\delta_{t_n} - 2), \cdots, \varphi(\delta_{t_n} - n_y)\}$, $\bar{\Phi}_{\delta_{t_n}} = I - \Phi_{\delta_{t_n}}$.

C. Description of RADoS Attacks

From a realistic perspective, malicious attackers may unexpectedly block data transmission in the shared network medium. In addition, it should be mentioned that attackers are hard to block communication for a long time under energy constraints. And it is also difficult for us to accurately predict the attacker's behavior. Hence, the RADoS attacks are considered in this article. In view of [37], the RADoS attacks are modeled by a Bernoulli process with the random variable $\sigma(l) \in \{0, 1\}$ and the probability distribution can be represented by

$$Prob\{\sigma(l) = 1\} = \bar{\sigma}, \; Prob\{\sigma(l) = 0\} = 1 - \bar{\sigma} \tag{9}$$

where $\bar{\sigma} = E\{\sigma(l)\} \in (0, 1)$ denotes a prescribed constant.

It is worth noting that RADoS attacks appear if and only if $\sigma(l) = 0$. Once it occurs, the transmitted signals will be blocked and the observer will not be capable to obtain useful information. In this scenario, the control performance may be affected to a certain extent. Therefore, ZOH approach is utilized to compensate the unselected sensor nodes posed by the SC protocol scheduling and the impact of RADoS attacks. Under the observation above, the updating law (7) is restated as follows:

$$\bar{y}_\hbar(t_n) = \begin{cases} \sigma(t_n) y_\hbar(t_n) + (1 - \sigma(t_n)) \bar{y}_\hbar(t_{n-1}), & \text{if } \hbar = \delta_{t_n} \\ \bar{y}_\hbar(t_{n-1}), & \text{otherwise.} \end{cases} \tag{10}$$

According to the formulas (8) and (10), it can be explicitly derived that

$$\begin{aligned} \bar{y}(t_n) = & \, \sigma(t_n) \Phi_{\delta_{t_n}} y(t_n) + (1 - \sigma(t_n)) \Phi_{\delta_{t_n}} \bar{y}(t_{n-1}) \\ & + \bar{\Phi}_{\delta_{t_n}} \bar{y}(t_{n-1}). \end{aligned} \tag{11}$$

D. OR Observer-Based Non-Fragile Controller

Due to the existence of measurement outliers, the performance of the observer may be deteriorated if the outliers are inappropriately tackled. To lessen the negative impacts of measurement outliers, the following OR fuzzy observer with m rules is considered:

RULE r: **IF** $\varsigma_1(\hat{x}(l))$**is**$\mathcal{W}_1^r$, $\varsigma_2(\hat{x}(l))$**is**$\mathcal{W}_2^r$, $\cdots$, $\varsigma_q(\hat{x}(l))$**is**$\mathcal{W}_q^r$, **THEN**

$$\begin{cases} \hat{x}(l+1) = A_r \hat{x}(l) + B_r u(l) + L_r sat(\bar{y}(t_n) - \hat{y}(l)) \\ \hat{y}(l) = C_{1r} \hat{x}(l) \end{cases} \tag{12}$$

where $\hat{x}(l) \in \mathbb{R}^{n_x}$, $\hat{y}(l) \in \mathbb{R}^{n_y}$ and L_r $(r = 1, 2, \cdots, m)$ denote the observer state vector, the measured output of the observer and the OR observer gain matrices to be designed, respectively. The saturation function $sat(\nu) = [sat_1^T(\nu_1) \;\; sat_2^T(\nu_2) \;\; \cdots \;\; sat_{n_y}^T(\nu_{n_y})]^T$ satisfies $sat_b(\nu_b) = sign(\nu_b) min\{\nu_{b,max}, |\nu_b|\}$ $(b = 1, 2, \cdots, n_y)$. $\nu_{b,max}$ stands for the b-th element of the saturation level ν_{max}. Subsequently, the following OR fuzzy observer can be represented:

$$\begin{cases} \hat{x}(l+1) = \sum_{r=1}^{m} \mu_r(\hat{x}(l)) [A_r \hat{x}(l) + B_r u(l) \\ \quad + L_r sat(\bar{y}(t_n) - \hat{y}(l))] \\ \hat{y}(l) = \sum_{r=1}^{m} \mu_r(\hat{x}(l)) C_{1r} \hat{x}(l). \end{cases} \tag{13}$$

Remark 3: The mentioned measurement outliers [31] mean that the witnessed values deviate from the normal situation. As illustrated in [34], the originated reasons can be generally concluded as the environmental variation, sensor failures, and cyber attacks. To maintain the fine effect of the observer, a saturation function $sat(\cdot)$ is utilized to restrict the specific range, which is predetermined by prior knowledge in practical implementations. Hence, the applied OR observer can decrease the adverse conditions brought by measurement outliers in contrast to the traditional fuzzy observer [7].

In control engineering applications, the phenomenon of uncertainties and perturbations is usually encountered and may lead to the controlled plant instability. To solve such a problem, the IT-2 fuzzy non-fragile controller with m rules is modeled as follows:

RULE h: **IF** $\varrho_1(\hat{x}(l))$**is**$\mathcal{N}_1^h$, $\varrho_2(\hat{x}(l))$**is**$\mathcal{N}_2^h$, $\cdots$, $\varrho_\epsilon(\hat{x}(l))$**is**$\mathcal{N}_\epsilon^h$, **THEN**

$$u(l) = (K_h + \Delta K_h(l))\hat{x}(l) \tag{14}$$

where $\mathcal{N}_c^h$ ($c = 1, 2, \cdots, \epsilon$ and $h = 1, 2, \cdots, m$) represents the fuzzy sets in line with the premise variable $\varrho_c(\hat{x}(l))$. The positive scalar ϵ is the quantity of the fuzzy sets. $K_h \in \mathbb{R}^{n_u \times n_x}$ denotes the h-th controller gain matrix to be devised. $\Delta K_h(l)$ symbolizes the time-varying parameter variations and its form can be assumed as follows:

$$\Delta K_h(l) = R_h \Delta_h(l) N_h \tag{15}$$

where R_h and N_h are given constant matrices. $\Delta_h(l)$ is unidentified matrix with the constraint $\Delta_h^T(l)\Delta_h(l) \leq I$.

On the ground of the content above, the following firing strength of the h-th fuzzy rule is given:

$$\tilde{\vartheta}_h(\hat{x}(l)) = [\underline{\vartheta}_h(\hat{x}(l)), \overline{\vartheta}_h(\hat{x}(l))] \tag{16}$$

where

$$\underline{\vartheta}_h(\hat{x}(l)) = \prod_{c=1}^{\epsilon} \underline{u}_{\mathcal{N}_c^h}(\varrho_c(\hat{x}(l))), \overline{\vartheta}_h(\hat{x}(l)) = \prod_{c=1}^{\epsilon} \overline{u}_{\mathcal{N}_c^h}(\varrho_c(\hat{x}(l))).$$

$\underline{u}_{\mathcal{N}_c^h}(\varrho_c(\hat{x}(l)))$ and $\overline{u}_{\mathcal{N}_c^h}(\varrho_c(\hat{x}(l)))$ represent LUMFs with $\overline{u}_{\mathcal{N}_c^h}(\varrho_c(\hat{x}(l))) \geq \underline{u}_{\mathcal{N}_c^h}(\varrho_c(\hat{x}(l))) \geq 0$. $\underline{\vartheta}_h(\hat{x}(l))$ and $\overline{\vartheta}_h(\hat{x}(l))$ are the lower and upper grades with $\overline{\vartheta}_h(\hat{x}(l)) \geq \underline{\vartheta}_h(\hat{x}(l)) \geq 0$. Afterwards, the IT-2 fuzzy non-fragile controller can be elicited as

$$u(l) = \sum_{h=1}^{m} \vartheta_h(\hat{x}(l))(K_h + \Delta K_h(l))\hat{x}(l) \tag{17}$$

where $\vartheta_h(\hat{x}(l)) = \hat{\vartheta}_h(\hat{x}(l))/\sum_{h=1}^{m}\hat{\vartheta}_h(\hat{x}(l))$, $\hat{\vartheta}_h(\hat{x}(l)) = \underline{\beta}_h(\hat{x}(l))\underline{\vartheta}_h(\hat{x}(l)) + \overline{\beta}_h(\hat{x}(l))\overline{\vartheta}_h(\hat{x}(l))$. $\vartheta_h(\hat{x}(l))$ denotes the normalized membership with $\sum_{h=1}^{m}\vartheta_h(\hat{x}(l)) = 1$. The nonlinear weighting functions $\underline{\beta}_h(\hat{x}(l)) \in [0, 1]$ and $\overline{\beta}_h(\hat{x}(l)) \in [0, 1]$ satisfy $\underline{\beta}_h(\hat{x}(l)) + \overline{\beta}_h(\hat{x}(l)) = 1$.

E. The Augmented IT-2 Fuzzy Model

Under the saturation function $sat(\cdot)$ in the OR observer (13), it is hard to directly obtain the augmented IT-2 fuzzy system. In an effort to overcome this obstacle, we assume that the function $sat(\cdot)$ [38] can be presented as

$$sat(\bar{y}(t_n) - \hat{y}(l)) = \mathcal{H}_1(\bar{y}(t_n) - \hat{y}(l)) + f(\bar{y}(t_n) - \hat{y}(l)) \tag{18}$$

where $\mathcal{H}_1$ is a diagonal matrix with $0 \leq \mathcal{H}_1 < I \leq \mathcal{H}_2$, from which $\mathcal{H}_2$ is an auxiliary matrix. $f(\bar{y}(t_n) - \hat{y}(l))$ denotes the nonlinear component. For the purpose of demonstrating the restrictive condition of the nonlinear component, the following definition is presented.

Definition 1: [38]: For real matrices $\mathcal{K}_1$, $\mathcal{K}_2$ with appropriate dimensions and positive-definite matrix $\mathcal{K} = \mathcal{K}_2 - \mathcal{K}_1$, a nonlinear function $f(\cdot)$ belongs to the sector $[\mathcal{K}_1, \mathcal{K}_2]$ if the following inequality holds:

$$(f(s) - \mathcal{K}_1 s)^T (f(s) - \mathcal{K}_2 s) \leq 0. \tag{19}$$

By applying Definition 1, when the parameters $\mathcal{K}_1 = 0$ and $\mathcal{K}_2 = \mathcal{H} \triangleq \mathcal{H}_2 - \mathcal{H}_1$, the following formula can be inferred:

$$E\{f^T(\bar{y}(t_n) - \hat{y}(l))[f(\bar{y}(t_n) - \hat{y}(l)) - \mathcal{H}(\bar{y}(t_n) - \hat{y}(l))]\} \leq 0. \tag{20}$$

In what follows, the augmented IT-2 fuzzy dynamics under the proposed MVET-SC protocol and RADoS attacks will be constructed. For brevity, δ_{t_n}, $\delta_{t_{n+1}}$ and $f(\bar{y}(t_n) - \hat{y}(l))$ are denoted by t, s and f_l, respectively. Meanwhile, we define $e(l) = x(l) - \hat{x}(l)$ as the estimation error.

According to the global IT-2 fuzzy model (3), the condition (11) and the non-fragile secure control law (17), we can comfortably derive that

$$\begin{aligned} x(l+1) = &\sum_{p=1}^{m}\sum_{h=1}^{m} \mu_p(x(l))\vartheta_h(\hat{x}(l))[(A_p + B_p K_h \\ &+ B_p \Delta K_h(l))\hat{x}(l) + A_p e(l) + B_{wp} w(l)] \end{aligned} \tag{21}$$

$$\begin{aligned} \bar{y}(t_n) = &\sum_{p=1}^{m} \mu_p(x(l))[\sigma(t_n)\Phi_t C_{1p}\hat{x}(l) + \sigma(t_n)\Phi_t C_{1p} e(l) \\ &+ (1 - \sigma(t_n))\Phi_t \bar{y}(t_{n-1}) + \bar{\Phi}_t \bar{y}(t_{n-1}) \\ &- \sigma(t_n)\Phi_t e_M(l)] \end{aligned} \tag{22}$$

$$z(l) = \sum_{p=1}^{m} \mu_p(x(l))[C_{2p}\hat{x}(l) + C_{2p} e(l)]. \tag{23}$$

In light of the OR fuzzy observer (13), the expressions (17) and (22), one has

$$\begin{aligned} \hat{x}(l+1) = &\sum_{p=1}^{m}\sum_{r=1}^{m}\sum_{h=1}^{m} \mu_p(x(l))\mu_r(\hat{x}(l))\vartheta_h(\hat{x}(l)) \\ &\times [(A_r + B_r K_h + B_r \Delta K_h(l) + \sigma(t_n) L_r \mathcal{H}_1 \Phi_t C_{1p} \\ &- L_r \mathcal{H}_1 C_{1r})\hat{x}(l) + \sigma(t_n) L_r \mathcal{H}_1 \Phi_t C_{1p} e(l) \\ &+ (1 - \sigma(t_n)) L_r \mathcal{H}_1 \Phi_t \bar{y}(t_{n-1}) + L_r \mathcal{H}_1 \bar{\Phi}_t \bar{y}(t_{n-1}) \\ &- \sigma(t_n) L_r \mathcal{H}_1 \Phi_t e_M(l) + L_r f_l]. \end{aligned} \tag{24}$$

By means of the formulas (21) and (24), it is simple to deduce that

$$\begin{aligned} e(l+1) = &\sum_{p=1}^{m}\sum_{r=1}^{m}\sum_{h=1}^{m} \mu_p(x(l))\mu_r(\hat{x}(l))\vartheta_h(\hat{x}(l)) \\ &\times [(A_p - A_r + B_p K_h - B_r K_h + B_p \Delta K_h(l) \\ &- B_r \Delta K_h(l) - \sigma(t_n) L_r \mathcal{H}_1 \Phi_t C_{1p} + L_r \mathcal{H}_1 C_{1r}) \\ &\times \hat{x}(l) + (A_p - \sigma(t_n) L_r \mathcal{H}_1 \Phi_t C_{1p}) e(l) \\ &- (1 - \sigma(t_n)) L_r \mathcal{H}_1 \Phi_t \bar{y}(t_{n-1}) - L_r \mathcal{H}_1 \bar{\Phi}_t \bar{y}(t_{n-1}) \\ &+ \sigma(t_n) L_r \mathcal{H}_1 \Phi_t e_M(l) - L_r f_l + B_{wp} w(l)]. \end{aligned} \tag{25}$$

Defining $\xi(l) = [\hat{x}^T(l)\ e^T(l)\ \bar{y}^T(t_{n-1})]^T$, the following augmented IT-2 fuzzy system is constructed:

$$\begin{cases} \xi(l+1) = \sum_{p=1}^{m}\sum_{r=1}^{m}\sum_{h=1}^{m}\mu_p(x(l))\mu_r(\hat{x}(l))\vartheta_h(\hat{x}(l)) \\ \quad [(\mathcal{F}_{1prht} + \mathcal{F}_{2prht})\xi(l) + \bar{B}_{wp}w(l) \\ \quad +(\mathcal{F}_{3prht} + \mathcal{F}_{4prht})e_M(l) + \mathcal{F}_{5r}f_l] \\ z(l) = \sum_{p=1}^{m}\mu_p(x(l))\bar{C}_{2p}\xi(l) \end{cases} \tag{26}$$

where

$$\mathcal{F}_{1prht} = \begin{bmatrix} \mathcal{F}_{11}^1 & \bar{\sigma}\Pi_{prt} & \mathcal{F}_{13}^1 \\ \mathcal{F}_{21}^1 & \mathcal{F}_{22}^1 & \mathcal{F}_{23}^1 \\ \bar{\sigma}\Phi_t C_{1p} & \bar{\sigma}\Phi_t C_{1p} & \mathcal{F}_{33}^1 \end{bmatrix},$$

$$\mathcal{F}_{2prht} = \begin{bmatrix} \tilde{\sigma}(t_n)\Pi_{prt} & \tilde{\sigma}(t_n)\Pi_{prt} & -\tilde{\sigma}(t_n)L_r\mathcal{H}_1\Phi_t \\ -\tilde{\sigma}(t_n)\Pi_{prt} & -\tilde{\sigma}(t_n)\Pi_{prt} & \tilde{\sigma}(t_n)L_r\mathcal{H}_1\Phi_t \\ \tilde{\sigma}(t_n)\Phi_t C_{1p} & \tilde{\sigma}(t_n)\Phi_t C_{1p} & -\tilde{\sigma}(t_n)\Phi_t \end{bmatrix},$$

$$\mathcal{F}_{3prht} = \begin{bmatrix} -\bar{\sigma}\Phi_t^T\mathcal{H}_1^T L_r^T & \bar{\sigma}\Phi_t^T\mathcal{H}_1^T L_r^T & -\bar{\sigma}\Phi_t^T \end{bmatrix}^T,$$

$$\mathcal{F}_{4prht} = \begin{bmatrix} -\tilde{\sigma}(t_n)\Phi_t^T\mathcal{H}_1^T L_r^T & \tilde{\sigma}(t_n)\Phi_t^T\mathcal{H}_1^T L_r^T & -\tilde{\sigma}(t_n)\Phi_t^T \end{bmatrix}^T,$$

$$\mathcal{F}_{5r} = \begin{bmatrix} L_r^T & -L_r^T & 0 \end{bmatrix}^T, \quad \bar{B}_{wp} = \begin{bmatrix} 0 & B_{wp}^T & 0 \end{bmatrix}^T,$$

$$\bar{C}_{2p} = \begin{bmatrix} C_{2p} & C_{2p} & 0 \end{bmatrix}, \quad \tilde{\sigma}(t_n) = \sigma(t_n) - \bar{\sigma},$$

$$\mathcal{F}_{11}^1 = A_r + B_r(K_h + \Delta K_h(l)) + L_r\mathcal{H}_1(\bar{\sigma}\Phi_t C_{1p} - C_{1r}),$$

$$\mathcal{F}_{13}^1 = \vec{\sigma}L_r\mathcal{H}_1\Phi_t + L_r\mathcal{H}_1\bar{\Phi}_t, \quad \Pi_{prt} = L_r\mathcal{H}_1\Phi_t C_{1p},$$

$$\mathcal{F}_{21}^1 = A_p - A_r + B_p(K_h + \Delta K_h(l)) - B_r(K_h + \Delta K_h(l)) - \bar{\sigma}L_r\mathcal{H}_1\Phi_t C_{1p} + L_r\mathcal{H}_1 C_{1r},$$

$$\mathcal{F}_{22}^1 = A_p - \bar{\sigma}L_r\mathcal{H}_1\Phi_t C_{1p}, \quad \vec{\sigma} = 1 - \bar{\sigma},$$

$$\mathcal{F}_{23}^1 = -\vec{\sigma}L_r\mathcal{H}_1\Phi_t - L_r\mathcal{H}_1\bar{\Phi}_t, \quad \mathcal{F}_{33}^1 = \vec{\sigma}\Phi_t + \bar{\Phi}_t.$$

Under the aforesaid descriptions, the OR observer-based secure fuzzy controller design approach will be investigated for nonlinear NCSs (1) with RADoS attacks and MVET-SC protocol. Before proceeding, the following lemmas and proposition are outlined to facilitate the next analysis.

Lemma 1: *[39]:* Given positive-semidefinite matrix Θ and the matrices $\mathcal{M}_p$ $(p = 1, 2, \cdots, m)$, if the conditions $\sum_{p=1}^{m}\mu_p = 1$ and $\mu_p \in [0, 1]$ hold, then the following inequality can be obtained:

$$\left(\sum_{p=1}^{m}\mu_p\mathcal{M}_p\right)^T \Theta \left(\sum_{p=1}^{m}\mu_p\mathcal{M}_p\right) \le \sum_{p=1}^{m}\mu_p\mathcal{M}_p^T\Theta\mathcal{M}_p. \tag{27}$$

Lemma 2: *[40]:* Suppose that $\Psi = \Psi^T$, S, Q and $\Delta(l)$ are real matrices with proper dimensions and $\Delta(l)\Delta^T(l) \le I$. Then, $\Psi + sym\{S\Delta(l)Q\} < 0$ holds if a parameter $\varepsilon > 0$ exists such that

$$\Psi + \varepsilon^{-1}SS^T + \varepsilon Q^T Q < 0. \tag{28}$$

Lemma 3: *[41]:* For a given matrix $B \in \mathbb{R}^{n_1 \times n_2}$ with $\text{rank}(B) = n_1$, the expression $B = O[S\ 0]D^T$ with $OO^T = I$ and $DD^T = I$ can be derived by the singular value decomposition. Denoting matrices $Y > 0$, $Y_{11} \in \mathbb{R}^{n_1 \times n_1}$ and $Y_{22} \in \mathbb{R}^{(n_2-n_1)\times(n_2-n_1)}$, there exists $\bar{Y}$ such that $BY = \bar{Y}B$ if the following condition holds:

$$Y = D\begin{bmatrix} Y_{11} & * \\ 0 & Y_{22} \end{bmatrix}D^T. \tag{29}$$

Proposition 1: If there exist scalars $\theta_j > 0$ and $a_j > 0$, the positiveness of $\sum_{j=1}^{N}\frac{\theta_j}{a_j}\lambda_j(l)$ in (5) can be ensured for $\forall l \in [0, \infty)$ under the initial value $\lambda_j(0) \ge 0$.

Proof: For $\forall l \in [t_n, t_{n+1})$, it can be explicitly observed that no event is triggered and the following inequality holds:

$$\sum_{j=1}^{N}\frac{\theta_j}{a_j}\lambda_j(l) - \Xi(l) \ge 0. \tag{30}$$

On the basis of the iterative expression (5) related to the MIDVs and the inequality (30), we can obtain that

$$\begin{aligned}\sum_{j=1}^{N}\frac{\theta_j}{a_j}\lambda_j(l+1) &\ge \sum_{j=1}^{N}\frac{\theta_j}{a_j}\kappa_j\lambda_j(l) - \kappa_{min}\sum_{j=1}^{N}\frac{\theta_j}{a_j}\lambda_j(l) \\ &= \sum_{j=1}^{N}\frac{\theta_j}{a_j}(\kappa_j - \kappa_{min})\lambda_j(l).\end{aligned} \tag{31}$$

Owing to the positive scalars θ_j, a_j and the condition $\kappa_j > \kappa_{min}$, one has

$$\begin{aligned}\sum_{j=1}^{N}\frac{\theta_j}{a_j}\lambda_j(l+1) &\ge \sum_{j=1}^{N}\frac{\theta_j}{a_j}(\kappa_j - \kappa_{min})^2\lambda_j(l-1) \\ &\ge \cdots \\ &\ge \sum_{j=1}^{N}\frac{\theta_j}{a_j}(\kappa_j - \kappa_{min})^{l+1}\lambda_j(0).\end{aligned} \tag{32}$$

Hence, under the inequality $\lambda_j(0) \ge 0$, it is easily derived that $\sum_{j=1}^{N}\frac{\theta_j}{a_j}\lambda_j(l) \ge 0$ holds for $\forall l \in [0, \infty)$. The proof of Proposition 1 has been completed.

III. Main Results

In this part, the asymptotic stability in the sense of H_∞ performance will be firstly analyzed for the augmented fuzzy dynamics (26) subject to RADoS attacks. Taking non-fragile parameters (15) into account, the sufficient design criteria under the proposed MVET-SC protocol are given. At the same time, the gains of the OR observer and non-fragile controller will be solved by applying linear matrix inequalities.

Theorem 1: For given scalars $\rho_1 > 0$, $\rho_2 > 0$, $\gamma > 0$, $\bar{\sigma} \in (0, 1)$, the MVETS parameters $a_j > 0$, $\theta_j > 0$, $\varepsilon_M^1 \in (0, 1)$, $\varepsilon_M^2 \in (0, 1)$, $\kappa_j > \kappa_{min}$, the gain matrices L_r, K_h and the condition $\vartheta_h(\hat{x}(l)) - \tau_h\mu_h(\hat{x}(l)) > 0$ with $\tau_h > 0$, the asymptotic stability of the augmented fuzzy model (26) under RADoS attacks and MVET-SC protocol can be ensured if there exist slack matrix Λ, positive-definite matrices $P_t > 0$ and Θ such that the following constraints hold:

$$\bar{\Psi}_{prht} + \bar{\Psi}_{phrt} - 2\Lambda < 0, \ r \le h \tag{33}$$

$$\tau_h\bar{\Psi}_{prht} + \tau_r\bar{\Psi}_{phrt} - \tau_h\Lambda - \tau_r\Lambda + 2\Lambda < 0, \ r \le h \tag{34}$$

where

$$\bar{\Psi}_{prht} = \Psi_{prht} + \Upsilon_p,$$

$$\Psi_{prht} = \begin{bmatrix} \Psi_{11} & * & * & * & * \\ \Psi_{21} & \Psi_{22} & * & * & * \\ \Psi_{31} & \Psi_{32} & \Psi_{33} & * & * \\ \Psi_{41} & \Psi_{42} & \Psi_{43} & \Psi_{44} & * \\ 0 & 0 & 0 & 0 & \Psi_{55} \end{bmatrix},$$

$$\Upsilon_p = \mathrm{diag}\{\bar{C}_{2p}^T\bar{C}_{2p}, 0, 0, -\gamma^2 I, 0_N\},$$

$$\Psi_{11} = \mathcal{F}_{1prht}^T\bar{P}_t\mathcal{F}_{1prht} + \bar{\mathcal{F}}_{2prht}^T\bar{P}_t\bar{\mathcal{F}}_{2prht} - P_t + \bar{\kappa}(\varepsilon_M^1 + \varepsilon_M^2)\bar{C}_{1p}^T\Theta\bar{C}_{1p},$$

$$\Psi_{21} = \mathcal{F}_{3prht}^T\bar{P}_t\mathcal{F}_{1prht} + \bar{\mathcal{F}}_{4prht}^T\bar{P}_t\bar{\mathcal{F}}_{2prht} - \bar{\kappa}\varepsilon_M^2\Theta\bar{C}_{1p},$$

$$\Psi_{22} = \mathcal{F}_{3prht}^T\bar{P}_t\mathcal{F}_{3prht} + \bar{\mathcal{F}}_{4prht}^T\bar{P}_t\bar{\mathcal{F}}_{4prht} - \bar{\kappa}\Theta + \bar{\kappa}\varepsilon_M^2\Theta,$$

$$\Psi_{31} = \mathcal{F}_{5r}^T\bar{P}_t\mathcal{F}_{1prht} + G_{prt},\ \Psi_{32} = \mathcal{F}_{5r}^T\bar{P}_t\mathcal{F}_{3prht} - \rho_2\bar{\sigma}\mathcal{H}\Phi_t,$$

$$\Psi_{33} = \mathcal{F}_{5r}^T\bar{P}_t\mathcal{F}_{5r} - \rho_2 I,\ \Psi_{41} = \bar{B}_{wp}^T\bar{P}_t\mathcal{F}_{1prht},$$

$$\Psi_{42} = \bar{B}_{wp}^T\bar{P}_t\mathcal{F}_{3prht},\ \Psi_{43} = \bar{B}_{wp}^T\bar{P}_t\mathcal{F}_{5r},\ \Psi_{44} = \bar{B}_{wp}^T\bar{P}_t\bar{B}_{wp},$$

$$\Psi_{55} = \mathrm{diag}\left\{\frac{\theta_1}{a_1}(\kappa_1 + \rho_1 - 1)I, \cdots, \frac{\theta_N}{a_N}(\kappa_N + \rho_1 - 1)I\right\},$$

$$\bar{\mathcal{F}}_{2prht} = \begin{bmatrix} \breve{\sigma}\Pi_{prt} & \breve{\sigma}\Pi_{prt} & -\breve{\sigma}L_r\mathcal{H}_1\Phi_t \\ -\breve{\sigma}\Pi_{prt} & -\breve{\sigma}\Pi_{prt} & \breve{\sigma}L_r\mathcal{H}_1\Phi_t \\ \breve{\sigma}\Phi_t C_{1p} & \breve{\sigma}\Phi_t C_{1p} & -\breve{\sigma}\Phi_t \end{bmatrix},\ \breve{\sigma} = \sqrt{\bar{\sigma}\vec{\sigma}},$$

$$\bar{\mathcal{F}}_{4prht} = \begin{bmatrix} -\breve{\sigma}\Phi_t^T\mathcal{H}_1^T L_r^T & \breve{\sigma}\Phi_t^T\mathcal{H}_1^T L_r^T & -\breve{\sigma}\Phi_t^T \end{bmatrix}^T,$$

$$\bar{C}_{1p} = \begin{bmatrix} C_{1p} & C_{1p} & 0 \end{bmatrix},\ \bar{P}_t = \sum_{s=1}^{n_y}\zeta_{ts}P_s,\ \bar{\kappa} = \kappa_{min} + \rho_1,$$

$$G_{prt} = \begin{bmatrix} G_{11} & G_{12} & G_{13} \end{bmatrix},\ G_{11} = \rho_2\bar{\sigma}\mathcal{H}\Phi_t C_{1p} - \rho_2\mathcal{H}C_{1r},$$

$$G_{12} = \rho_2\bar{\sigma}\mathcal{H}\Phi_t C_{1p},\ G_{13} = \rho_2\vec{\sigma}\mathcal{H}\Phi_t + \rho_2\mathcal{H}\bar{\Phi}_t.$$

Proof: Based on MVET-SC protocol and Proposition 1, the following Lyapunov function is constructed:

$$V(l) = \xi^T(l)P_t\xi(l) + \sum_{j=1}^{N}\frac{\theta_j}{a_j}\lambda_j(l). \quad (35)$$

Combing the conditions (20) and (30), it is evidently inferred that

$$\begin{aligned} E\{\Delta V(l)\} &= E\{V(l+1) - V(l)\} \\ &\le E\{\xi^T(l+1)\bar{P}_t\xi(l+1) - \xi^T(l)P_t\xi(l) \\ &\quad + \sum_{j=1}^{N}\frac{\theta_j}{a_j}\lambda_j(l+1) - \sum_{j=1}^{N}\frac{\theta_j}{a_j}\lambda_j(l) \\ &\quad + \rho_1[\sum_{j=1}^{N}\frac{\theta_j}{a_j}\lambda_j(l) - \Xi(l)] \\ &\quad + \rho_2[-f_l^T f_l + f_l^T\mathcal{H}(\bar{y}(t_n) - \hat{y}(l))]\}. \end{aligned} \quad (36)$$

On the basis of Lemma 1, according to MVETS (5) and the augmented fuzzy system (26), we can derive

$$\begin{aligned} E\{\Delta V(l)\} &\le E\{\sum_{p=1}^{m}\sum_{r=1}^{m}\sum_{h=1}^{m}\mu_p(x(l))\mu_r(\hat{x}(l))\vartheta_h(\hat{x}(l)) \\ &\quad \times [(\mathcal{F}_{1prht} + \mathcal{F}_{2prht})\xi(l) + \bar{B}_{wp}w(l) \\ &\quad + (\mathcal{F}_{3prht} + \mathcal{F}_{4prht})e_M(l) + \mathcal{F}_{5r}f_l]^T\bar{P}_t \\ &\quad \times [(\mathcal{F}_{1prht} + \mathcal{F}_{2prht})\xi(l) + \bar{B}_{wp}w(l) \\ &\quad + (\mathcal{F}_{3prht} + \mathcal{F}_{4prht})e_M(l) + \mathcal{F}_{5r}f_l] \\ &\quad - \xi^T(l)P_t\xi(l) + \sum_{j=1}^{N}\frac{\theta_j}{a_j}(\kappa_j\lambda_j(l) - \theta_j\Xi(l)) \\ &\quad - \sum_{j=1}^{N}\frac{\theta_j}{a_j}\lambda_j(l) + \rho_1[\sum_{j=1}^{N}\frac{\theta_j}{a_j}\lambda_j(l) - \Xi(l)] \\ &\quad + \rho_2[-f_l^T f_l + f_l^T\mathcal{H}(\bar{y}(t_n) - \hat{y}(l))]\}. \end{aligned} \quad (37)$$

In view of the vector augmentation technique, we develop the condition (37) as

$$E\{\Delta V(l)\} \le \sum_{p=1}^{m}\sum_{r=1}^{m}\sum_{h=1}^{m}\mu_p(x(l))\mu_r(\hat{x}(l))\vartheta_h(\hat{x}(l)) \times \eta^T(l)\Psi_{prht}\eta(l) \quad (38)$$

where $\eta(l) = [\xi^T(l)\ e_M^T(l)\ f_l^T\ w^T(l)\ \sqrt{\lambda_1(l)}^T \cdots \sqrt{\lambda_N(l)}^T]^T$ stands for the augmented vector.

By virtue of the control output (26) and the condition (38), the following formula is obtained:

$$\begin{aligned} &E\{\Delta V(l)\} + E\{z^T(l)z(l) - \gamma^2 w^T(l)w(l)\} \\ &\le \sum_{p=1}^{m}\sum_{r=1}^{m}\sum_{h=1}^{m}\mu_p(x(l))\mu_r(\hat{x}(l))\vartheta_h(\hat{x}(l))\eta^T(l)\bar{\Psi}_{prht}\eta(l). \end{aligned} \quad (39)$$

Inspired by [42], the slack matrix Λ is utilized to reduce the conservatism of theoretical results and the condition can be deduced as follows:

$$\begin{aligned} &\sum_{p=1}^{m}\sum_{r=1}^{m}\sum_{h=1}^{m}\mu_p(x(l))\mu_r(\hat{x}(l))[(\mu_h(\hat{x}(l)) - \vartheta_h(\hat{x}(l)))\Lambda] \\ &= \sum_{p=1}^{m}\sum_{r=1}^{m}\mu_p(x(l))\mu_r(\hat{x}(l))[(\sum_{h=1}^{m}\mu_h(\hat{x}(l)) - \sum_{h=1}^{m}\vartheta_h(\hat{x}(l)))\Lambda] \\ &= 0. \end{aligned} \quad (40)$$

Taking the expression (39) and the zero term (40) into account, one has

$$\begin{aligned} &E\{\Delta V(l)\} + E\{z^T(l)z(l) - \gamma^2 w^T(l)w(l)\} \\ &\le \sum_{p=1}^{m}\sum_{r=1}^{m}\sum_{h=1}^{m}\mu_p(x(l))\mu_r(\hat{x}(l))\eta^T(l) \\ &\quad \times [(\vartheta_h(\hat{x}(l)) - \tau_h\mu_h(\hat{x}(l)))(\bar{\Psi}_{prht} - \Lambda) \\ &\quad + \mu_h(\hat{x}(l))(\tau_h\bar{\Psi}_{prht} - \tau_h\Lambda + \Lambda)]\eta(l) \\ &= \frac{1}{2}\sum_{p=1}^{m}\sum_{r=1}^{m}\sum_{h=1}^{m}\mu_p(x(l))\mu_r(\hat{x}(l))\eta^T(l) \\ &\quad \times [(\vartheta_h(\hat{x}(l)) - \tau_h\mu_h(\hat{x}(l)))(\bar{\Psi}_{prht} + \bar{\Psi}_{phrt} - 2\Lambda) \\ &\quad + \mu_h(\hat{x}(l))(\tau_h\bar{\Psi}_{prht} + \tau_r\bar{\Psi}_{phrt} - \tau_h\Lambda - \tau_r\Lambda + 2\Lambda)]\eta(l). \end{aligned} \quad (41)$$

Under the conditions (33) and (34), it can be readily conclude that

$$E\{\Delta V(l)\} + E\{z^T(l)z(l) - \gamma^2 w^T(l)w(l)\} \le 0. \quad (42)$$

Based on the method of Schur complement, $E\{\Delta V(l)\} \leq 0$ can be derived when the external disturbance $w(l) = 0$, and the asymptotic stability of the augmented IT-2 fuzzy system has been guaranteed. Additionally, we sum both sides of (42) from 0 to ∞, it yields

$$\sum_{k=0}^{\infty} E\left\{z^T(l)z(l)\right\} \leq \gamma^2 \sum_{k=0}^{\infty} w^T(l)w(l) \tag{43}$$

which demonstrates the satisfaction of H_∞ performance index. Thus, the proof of Theorem 1 is finished.

Theorem 2: Given parameters $\rho_1 > 0, \rho_2 > 0, \gamma > 0, a_j > 0$, $\theta_j > 0$, $\varepsilon_w > 0$ $(w = 1, 2, 3, 4)$, $\bar{\sigma} \in (0, 1)$, $\varepsilon_M^1 \in (0, 1)$, $\varepsilon_M^2 \in (0, 1)$, $\kappa_j > \kappa_{min}$ and the expression $\vartheta_h(\hat{x}(l)) - \tau_h \mu_h(\hat{x}(l)) > 0$ $(\tau_h > 0)$, the augmented fuzzy dynamics (26) subject to RADoS attacks becomes asymptotically stable if there exist matrices $Y > 0$, $P_t > 0$, U_r, U_h, V_r, V_h, slack matrix Λ and weight matrix Θ such that

$$\begin{bmatrix} -\varepsilon_2^{-1} I & * & * & * & * \\ 0 & -\varepsilon_2 I & * & * & * \\ 0 & 0 & -\varepsilon_1^{-1} I & * & * \\ 0 & 0 & 0 & -\varepsilon_1 I & * \\ Q_r^{1T} & \bar{S}_{rh}^1 & Q_h^{1T} & \bar{S}_{hr}^1 & \vec{\Psi}_{prht}^1 \end{bmatrix} < 0, \ r \leq h \tag{44}$$

$$\begin{bmatrix} -\varepsilon_4^{-1} I & * & * & * & * \\ 0 & -\varepsilon_4 I & * & * & * \\ 0 & 0 & -\varepsilon_3^{-1} I & * & * \\ 0 & 0 & 0 & -\varepsilon_3 I & * \\ Q_r^{2T} & \bar{S}_{rh}^2 & Q_h^{2T} & \bar{S}_{hr}^2 & \vec{\Psi}_{prht}^2 \end{bmatrix} < 0, \ r \leq h \tag{45}$$

with

$$L_r^T = U_r (Y^T)^{-1}, \quad K_h^T = V_h O S Y_{11}^{-1} S^{-1} O^{-1} \tag{46}$$

where the relevant parameters are presented in Appendix.

Proof: In the light of Schur complement lemma, (33) and (34) are equal to the following conditions:

$$\Psi_{prht}^1 = \begin{bmatrix} 2\mathcal{P}_t & * \\ \Sigma_{prht} + \Sigma_{phrt} & \mathcal{U} \end{bmatrix} < 0, \ r \leq h \tag{47}$$

$$\Psi_{prht}^2 = \begin{bmatrix} 2\mathcal{P}_t & * \\ \sqrt{\tau_h}\Sigma_{prht} + \sqrt{\tau_r}\Sigma_{phrt} & \mathcal{V} \end{bmatrix} < 0, \ r \leq h \tag{48}$$

in which

$$\mathcal{P}_t = \mathrm{diag}\{-\bar{P}_t^{-1}, -\bar{P}_t^{-1}, -I, -\Theta^{-1}, -\Theta^{-1}, -I_{N-1}\},$$
$$\bar{P}_t = \mathrm{diag}\{\bar{P}_{1,t}, \bar{P}_{2,t}, \bar{P}_{3,t}\},$$
$$\Sigma_{prht} = \begin{bmatrix} \mathcal{F}_{1prht}^T & \bar{\mathcal{F}}_{2prht}^T & \bar{C}_{2p}^T & \tilde{\varepsilon}_M^1 \bar{C}_{1p}^T & \tilde{\varepsilon}_M^2 \bar{C}_{1p}^T & 0_{N-1} \\ \mathcal{F}_{3prht}^T & \bar{\mathcal{F}}_{4prht}^T & 0 & 0 & -\tilde{\varepsilon}_M^2 I & 0_{N-1} \\ \mathcal{F}_{5r}^T & 0 & 0 & 0 & 0 & 0_{N-1} \\ \bar{B}_{wp}^T & 0 & 0 & 0 & 0 & 0_{N-1} \\ 0_N^T & 0_N^T & 0_N^T & 0_N^T & 0_N^T & 0_{N-1}^N \end{bmatrix}.$$

According to the non-fragile control parameters in (15), we can derive that

$$\Psi_{prht}^1 = \tilde{\Psi}_{prht}^1 + sym\{S_{hr}^1 \Delta_h(l) Q_h^1 + S_{rh}^1 \Delta_r(l) Q_r^1\} < 0 \tag{49}$$

$$\Psi_{prht}^2 = \tilde{\Psi}_{prht}^2 + sym\{S_{hr}^2 \Delta_h(l) Q_h^2 + S_{rh}^2 \Delta_r(l) Q_r^2\} < 0 \tag{50}$$

where

$$S_{hr}^{1T} = \begin{bmatrix} R_h^T B_r^T & R_h^T(B_p^T - B_r^T) & 0_{2N+12} \end{bmatrix}, \ S_{hr}^{2T} = S_{hr}^{1T},$$
$$\tilde{\Psi}_{prht}^1 = \begin{bmatrix} 2\mathcal{P}_t & * \\ \bar{\Sigma}_{prht} + \bar{\Sigma}_{phrt} & \mathcal{U} \end{bmatrix},$$
$$\tilde{\Psi}_{prht}^2 = \begin{bmatrix} 2\mathcal{P}_t & * \\ \sqrt{\tau_h}\bar{\Sigma}_{prht} + \sqrt{\tau_r}\bar{\Sigma}_{phrt} & \mathcal{V} \end{bmatrix},$$
$$\bar{\Sigma}_{prht} = \begin{bmatrix} \bar{\mathcal{F}}_{1prht}^T & \bar{\mathcal{F}}_{2prht}^T & \bar{C}_{2p}^T & \tilde{\varepsilon}_M^1 \bar{C}_{1p}^T & \tilde{\varepsilon}_M^2 \bar{C}_{1p}^T & 0_{N-1} \\ \mathcal{F}_{3prht}^T & \bar{\mathcal{F}}_{4prht}^T & 0 & 0 & -\tilde{\varepsilon}_M^2 I & 0_{N-1} \\ \mathcal{F}_{5r}^T & 0 & 0 & 0 & 0 & 0_{N-1} \\ \bar{B}_{wp}^T & 0 & 0 & 0 & 0 & 0_{N-1} \\ 0_N^T & 0_N^T & 0_N^T & 0_N^T & 0_N^T & 0_{N-1}^N \end{bmatrix},$$
$$\bar{\mathcal{F}}_{1prht} = \begin{bmatrix} \bar{\mathcal{F}}_{11}^1 & \bar{\sigma}\Pi_{prt} & \mathcal{F}_{13}^1 \\ \bar{\mathcal{F}}_{21}^1 & \mathcal{F}_{22}^1 & \mathcal{F}_{23}^1 \\ \bar{\sigma}\Phi_t C_{1p} & \bar{\sigma}\Phi_t C_{1p} & \mathcal{F}_{33}^1 \end{bmatrix},$$
$$\bar{\mathcal{F}}_{11}^1 = A_r + B_r K_h + L_r \mathcal{H}_1(\bar{\sigma}\Phi_t C_{1p} - C_{1r}),$$
$$\bar{\mathcal{F}}_{21}^1 = A_p - A_r + (B_p - B_r)K_h - L_r \mathcal{H}_1(\bar{\sigma}\Phi_t C_{1p} - C_{1r}).$$

On the ground of Lemma 2, (49) and (50), the following inequalities are obtained:

$$\tilde{\Psi}_{prht}^1 + \varepsilon_1^{-1} S_{hr}^1 S_{hr}^{1T} + \varepsilon_1 Q_h^{1T} Q_h^1 + \varepsilon_2^{-1} S_{rh}^1 S_{rh}^{1T} + \varepsilon_2 Q_r^{1T} Q_r^1 < 0 \tag{51}$$

$$\tilde{\Psi}_{prht}^2 + \varepsilon_3^{-1} S_{hr}^2 S_{hr}^{2T} + \varepsilon_3 Q_h^{2T} Q_h^2 + \varepsilon_4^{-1} S_{rh}^2 S_{rh}^{2T} + \varepsilon_4 Q_r^{2T} Q_r^2 < 0. \tag{52}$$

Then, on the basis of Schur complement, the conditions (51) and (52) are readily transformed as

$$\begin{bmatrix} -\varepsilon_2^{-1} I & * & * & * & * \\ 0 & -\varepsilon_2 I & * & * & * \\ 0 & 0 & -\varepsilon_1^{-1} I & * & * \\ 0 & 0 & 0 & -\varepsilon_1 I & * \\ Q_r^{1T} & S_{rh}^1 & Q_h^{1T} & S_{hr}^1 & \tilde{\Psi}_{prht}^1 \end{bmatrix} < 0 \tag{53}$$

$$\begin{bmatrix} -\varepsilon_4^{-1} I & * & * & * & * \\ 0 & -\varepsilon_4 I & * & * & * \\ 0 & 0 & -\varepsilon_3^{-1} I & * & * \\ 0 & 0 & 0 & -\varepsilon_3 I & * \\ Q_r^{2T} & S_{rh}^2 & Q_h^{2T} & S_{hr}^2 & \tilde{\Psi}_{prht}^2 \end{bmatrix} < 0. \tag{54}$$

Define auxiliary matrix $\mathcal{Y} = \mathrm{diag}\{I_4, Y_6, I, Y, Y, I_{2N+5}\}$. Multiplying the left and right sides of (53) and (54) by $\mathcal{Y}$ and $\mathcal{Y}^T$, it can be deduced that

$$\begin{bmatrix} -\varepsilon_2^{-1} I & * & * & * & * \\ 0 & -\varepsilon_2 I & * & * & * \\ 0 & 0 & -\varepsilon_1^{-1} I & * & * \\ 0 & 0 & 0 & -\varepsilon_1 I & * \\ Q_r^{1T} & \bar{S}_{rh}^1 & Q_h^{1T} & \bar{S}_{hr}^1 & \check{\Psi}_{prht}^1 \end{bmatrix} < 0 \tag{55}$$

$$\begin{bmatrix} -\varepsilon_4^{-1} I & * & * & * & * \\ 0 & -\varepsilon_4 I & * & * & * \\ 0 & 0 & -\varepsilon_3^{-1} I & * & * \\ 0 & 0 & 0 & -\varepsilon_3 I & * \\ Q_r^{2T} & \bar{S}_{rh}^2 & Q_h^{2T} & \bar{S}_{hr}^2 & \check{\Psi}_{prht}^2 \end{bmatrix} < 0 \tag{56}$$

where

$$\check{\Psi}^1_{prht} = \begin{bmatrix} 2\check{\mathcal{P}}_t & * \\ \check{\Sigma}_{prht} + \check{\Sigma}_{phrt} & \mathcal{U} \end{bmatrix},$$

$$\check{\Psi}^2_{prht} = \begin{bmatrix} 2\check{\mathcal{P}}_t & * \\ \sqrt{\tau_h}\check{\Sigma}_{prht} + \sqrt{\tau_r}\check{\Sigma}_{phrt} & \mathcal{V} \end{bmatrix},$$

$$\check{\mathcal{P}}_t = \text{diag}\{-Y\bar{P}_t^{-1}Y^T, -Y\bar{P}_t^{-1}Y^T, -I, -Y\Theta^{-1}Y^T, -Y\Theta^{-1}Y^T, -I_{N-1}\},$$

$$\check{\Sigma}_{prht} = \begin{bmatrix} \check{\mathcal{F}}^T_{1prht} & \tilde{\mathcal{F}}^T_{2prht} & \bar{C}^T_{2p} & \tilde{C}^{1T}_{1p} & \tilde{C}^{2T}_{1p} & 0_{N-1} \\ \check{\mathcal{F}}^T_{3prht} & \tilde{\mathcal{F}}^T_{4prht} & 0 & 0 & -\tilde{\varepsilon}^2_M Y^T & 0_{N-1} \\ \check{\mathcal{F}}^T_{5r} & 0 & 0 & 0 & 0 & 0_{N-1} \\ \check{B}^T_{wp} & 0 & 0 & 0 & 0 & 0_{N-1} \\ 0^T_N & 0^T_N & 0^T_N & 0^T_N & 0^T_N & 0^N_{N-1} \end{bmatrix},$$

$$\check{\mathcal{F}}^T_{1prht} = \begin{bmatrix} \check{\mathcal{F}}^1_{11} & \check{\mathcal{F}}^1_{12} & \bar{\sigma}C^T_{1p}\Phi^T_t Y^T \\ \bar{\sigma}C^T_{1p}\Phi^T_t\mathcal{H}^T_1 U_r & \check{\mathcal{F}}^1_{22} & \bar{\sigma}C^T_{1p}\Phi^T_t Y^T \\ \check{\mathcal{F}}^1_{31} & \check{\mathcal{F}}^1_{32} & \bar{\sigma}\Phi^T_t Y^T + \bar{\Phi}^T_t Y^T \end{bmatrix},$$

$$\check{\mathcal{F}}^1_{11} = A^T_r Y^T + K^T_h B^T_r Y^T + \bar{\sigma}C^T_{1p}\Phi^T_t\mathcal{H}^T_1 U_r - C^T_{1r}\mathcal{H}^T_1 U_r,$$

$$\check{\mathcal{F}}^1_{12} = A^T_p Y^T - A^T_r Y^T + K^T_h B^T_p Y^T - K^T_h B^T_r Y^T - \bar{\sigma}C^T_{1p}\Phi^T_t\mathcal{H}^T_1 U_r + C^T_{1r}\mathcal{H}^T_1 U_r.$$

With the help of $(\bar{P}_{\iota,t} - Y)\bar{P}^{-1}_{\iota,t}(\bar{P}_{\iota,t} - Y)^T \geq 0$ $(\iota = 1, 2, 3)$, we can get

$$-Y\bar{P}^{-1}_{\iota,t}Y^T \leq \bar{P}_{\iota,t} - sym\{Y\}. \tag{57}$$

At the same time, one has

$$-Y\Theta^{-1}Y^T \leq \Theta - sym\{Y\}. \tag{58}$$

Similar to [43], the matrices B^T_r, B^T_h and B^T_p are assumed to become common one and it is represented as B^T. Hence, based on Lemma 3, the matrix $B^T = O[S \ \ 0]D^T$ with $OO^T = I$ and $DD^T = I$. For $Y = D\begin{bmatrix} Y_{11} & * \\ 0 & Y_{22} \end{bmatrix}D^T$, one has $B^T Y^T = \bar{Y}^T B^T$ with $\bar{Y}^T = OSY_{11}S^{-1}O^{-1}$. Then, we define $V_h = K^T_h\bar{Y}^T$ and the conditions (44) and (45) can be obtained by considering (57) and (58). What is more, it should be mentioned that the sufficient criteria (33) and (34) in Theorem 1 can be guaranteed by (44) and (45). Meanwhile, the gain matrices of OR observer and non-fragile controller are derived as $L^T_r = U_r(Y^T)^{-1}$, $K^T_h = V_h OSY^{-1}_{11}S^{-1}O^{-1}$. The proof of Theorem 2 is completed.

IV. Simulation Example

In this position, a mass-spring-damping system (MSDS) borrowed from [37] is utilized to exemplify the effectiveness of the OR observer-based control strategy under RADoS attacks and MVET-SC protocol. On account of the Newton's second law, the corresponding dynamics can be modeled as

$$M\ddot{x} = u(t) - F_f - F_s \tag{59}$$

where M, x, $u(t)$, F_f and F_s represent the mass, the displacement, the control input, the frictional force and the spring restoring force, respectively. Define $F_f = c_b\dot{x}$ and $F_s = k_b x + k_b a^2 x^3$ with $c_b > 0$ being the friction coefficient. Subsequently, the MSDS is rewritten as

$$M\ddot{x} = u(t) - c_b\dot{x} - k_b x - k_b a^2 x^3. \tag{60}$$

Denote the auxiliary function $\psi(k_b, t) = \frac{-k_b - k_b a^2 x_1^2(t)}{M}$ and $x(t) = [x_1^T(t) \ \ x_2^T(t)]^T$ with $x_1(t) = x$, $x_2(t) = \dot{x}$. Then, by assuming $x_1(t) \in [-2, 2]$, $k_b \in [\underline{k}_b, \bar{k}_b]$, $\underline{k}_b = 4N/m$, $\bar{k}_b = 7N/m$, $M = 0.5kg$, $c_b = 1.95N\cdot m/s$ and $a = 0.05m^{-1}$, it can be derived that $\psi_{min} = -14.14$ $(k_b = \bar{k}_b,\ x_1(t) = \pm 2)$ and $\psi_{max} = -8$ $(k_b = \underline{k}_b,\ x_1(t) = 0)$. In light of the T-S fuzzy approach in [44], the following LUMFs are derived:

$$\underline{\chi}_1(x_1(t)) = \frac{\psi_{max} - \psi(\underline{k}_b, t)}{\psi_{max} - \psi_{min}},\ \ \bar{\chi}_1(x_1(t)) = \frac{\psi_{max} - \psi(\bar{k}_b, t)}{\psi_{max} - \psi_{min}}$$

$$\underline{\chi}_2(x_1(t)) = \frac{\psi(\bar{k}_b, t) - \psi_{min}}{\psi_{max} - \psi_{min}},\ \ \bar{\chi}_2(x_1(t)) = \frac{\psi(\underline{k}_b, t) - \psi_{min}}{\psi_{max} - \psi_{min}}.$$

According to the Euler's discretization technique, by adopting the sampling period $h_s = 0.1s$, the coefficient matrices of the plant (1) are presented as

$$A_1 = I + h_s\begin{bmatrix} 0 & 1 \\ \psi_{min} & -\frac{c_b}{M} \end{bmatrix},\quad B_1 = h_s\begin{bmatrix} 0 \\ \frac{1}{M} \end{bmatrix}$$

$$A_2 = I + h_s\begin{bmatrix} 0 & 1 \\ \psi_{max} & -\frac{c_b}{M} \end{bmatrix},\quad B_2 = h_s\begin{bmatrix} 0 \\ \frac{1}{M} \end{bmatrix}$$

and other related parameters are defined as

$$C_{11} = \begin{bmatrix} 0.1 & 0 \\ 0 & 0.1 \end{bmatrix},\quad B_{w1} = \begin{bmatrix} 0.012 \\ 0.208 \end{bmatrix},\quad R_1 = 0.14$$

$$C_{12} = \begin{bmatrix} 0.1 & 0 \\ 0 & 0.1 \end{bmatrix},\quad B_{w2} = \begin{bmatrix} 0.015 \\ 0.134 \end{bmatrix},\quad R_2 = 0.27$$

$$C_{21} = \begin{bmatrix} 0.07 & 0.02 \end{bmatrix},\quad N_1 = \begin{bmatrix} 0.126 & 0.051 \end{bmatrix}$$

$$C_{22} = \begin{bmatrix} 0.11 & 0.08 \end{bmatrix},\quad N_2 = \begin{bmatrix} 0.168 & 0.083 \end{bmatrix}.$$

TABLE I

LUMFs of the Secure Controller

Lower membership functions	Upper membership functions
$\underline{\vartheta}_1(\hat{x}(l)) = 1 - 0.35e^{-\hat{x}_1^2(l)}$	$\bar{\vartheta}_1(\hat{x}(l)) = \underline{\vartheta}_1(\hat{x}(l))$
$\underline{\vartheta}_2(\hat{x}(l)) = 0.35e^{-\hat{x}_1^2(l)}$	$\bar{\vartheta}_2(\hat{x}(l)) = \underline{\vartheta}_2(\hat{x}(l))$

Meanwhile, the LUMFs of the secure controller are presented in TABLE I, and the following nonlinear weighting functions can be selected:

$$\underline{\alpha}_p(x(l)) = 0.55cos^2(x_1(l)),\quad \bar{\alpha}_p(x(l)) = 1 - \underline{\alpha}_p(x(l))$$

$$\underline{\beta}_h(\hat{x}(l)) = sin^2(\hat{x}_1(l)),\quad \bar{\beta}_h(\hat{x}(l)) = 1 - \underline{\beta}_h(\hat{x}(l)).$$

Let the parameters of MVET-SC protocol $N = 2$, $a_1 = 20$, $a_2 = 5$, $\theta_1 = 0.4$, $\theta_2 = 0.6$, $\varepsilon^1_M = 0.12$, $\varepsilon^2_M = 0.08$, $\kappa_1 = \kappa_2 = 0.3$, $\zeta_{11} = 0.75$, $\zeta_{12} = 0.25$, $\zeta_{21} = 0.35$, $\zeta_{22} = 0.65$ and the scalars $\rho_1 = 0.15$, $\rho_2 = 0.025$, $\varepsilon_1 = 0.054$, $\varepsilon_2 = 0.068$, $\varepsilon_3 = 0.032$, $\varepsilon_4 = 0.081$, $\tau_1 = 0.96$, $\tau_2 = 0.48$. Under the probability $\bar{\sigma} = 0.25$ related to RADoS attacks and the H_∞ performance index $\gamma = 0.32$, the OR observer gains and the non-fragile secure controller gains are solved as

$$L_1 = \begin{bmatrix} 0.0006 & 0.0025 \\ 0.0035 & 0.0062 \end{bmatrix},\quad L_2 = \begin{bmatrix} -0.0004 & 0.0012 \\ 0.0061 & -0.0116 \end{bmatrix}$$

$$K_1 = \begin{bmatrix} 3.3566 & -3.2535 \end{bmatrix},\quad K_2 = \begin{bmatrix} 0.3336 & -3.3201 \end{bmatrix}$$

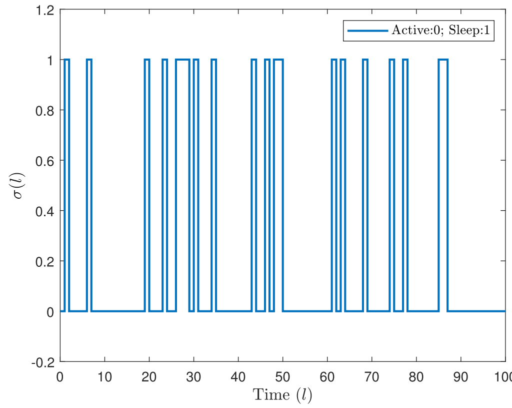

Fig. 2. The evolution of RADoS attacks.

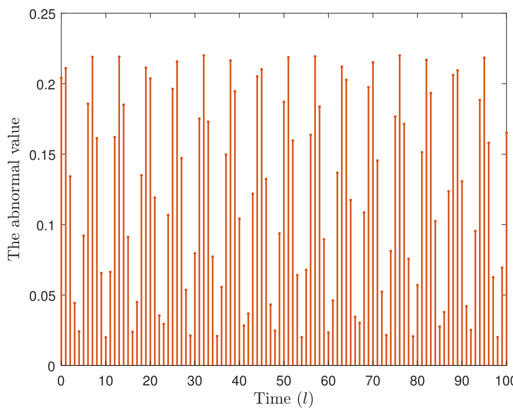

Fig. 3. The abnormal interference signals.

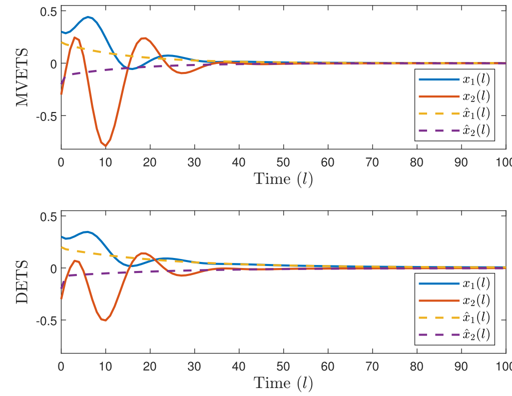

Fig. 4. The system states and estimations under different ETSs.

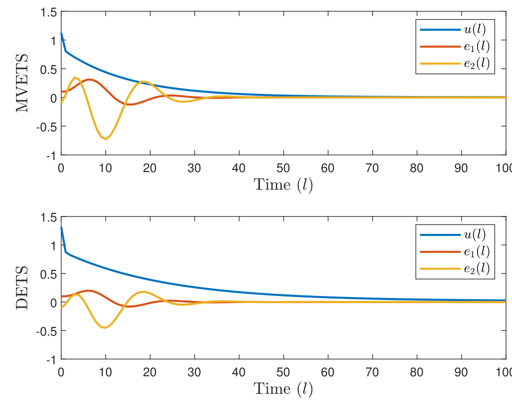

Fig. 5. The control input and estimation error under different ETSs.

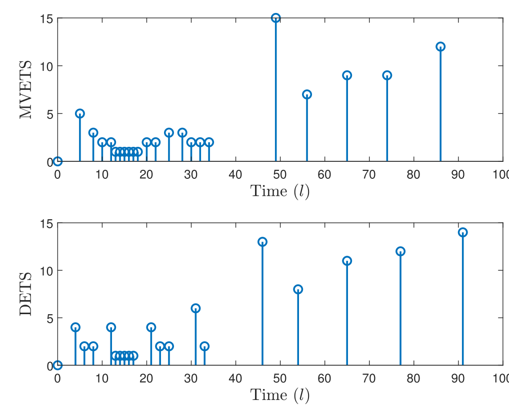

Fig. 6. The release instants of DETS and MVETS.

and the weight matrix in MVET-SC protocol can be simultaneously computed as

$$\Theta = \begin{bmatrix} 6.0406 & 0.5142 \\ 0.5142 & 0.4745 \end{bmatrix}.$$

When the measured output $y(t_n)$ is transmitted via an open communication network, the malicious adversary may block the transmission process in a random pattern. The signals of RADoS attacks are given in Fig. 2. Meanwhile, under the consideration of the measured outliers, Fig. 3 displays the abnormal signals added to the measured output between the sensors and the OR observer. The external interference $w(l)$ in (1) is set to be $2.5e^{-0.2l}sin(0.4l)$. Based on the above factors, we will next demonstrate the validity of the MVET-SC protocol and the secure fuzzy control scheme against RADoS attacks.

In what follows, the convergence of system stability is expounded by comparing some results under MVETS and DETS in [35]. With the initial states $x(0) = [0.3 \quad -0.3]^T$ and $\hat{x}(0) = [0.2 \ -0.2]^T$, Fig. 4 depicts the trajectories of the system states $x_1(l)$, $x_2(l)$ and the corresponding estimations subject to RADoS attacks. It is apparently observed that the system states gradually tend to be stable as time goes by and the better system performance can be attained under MVETS. To be specific, the MVETS-based and DETS-based system states converge to zero about 55 and 71 time instant, respectively. In addition, the trajectories of the control input $u(l)$ and the estimation error $e_1(l)$, $e_2(l)$ are presented in Fig. 5. In comparison with DETS, the control input in the presence of MVETS can also reach the stable condition at a faster speed, which illustrate the validity of the proposed secure control policy under MVET-SC protocol.

On the other hand, the quantity of triggered data packets should also be concerned so as to validate the relevant descriptions in Remark 1. Fig. 6 presents the triggered instants generated by the aforementioned ETS. Based on the initial value $\lambda(0) = \lambda_1(0) = 1$ and $\lambda_2(0) = 0.5$, the curves of IDV $\lambda(l)$ in [35] and MIDVs $\lambda_j(l)$ in (5) are shown in Fig. 7. It is explicitly witnessed that the differences in the number of triggered data packets are not evident. Specifically, the total number of triggered instants within 100 time instants is 23 in MVETS and 20 in DETS, respectively. Furthermore, the ET dynamicity can be vividly characterized by MIDVs rather

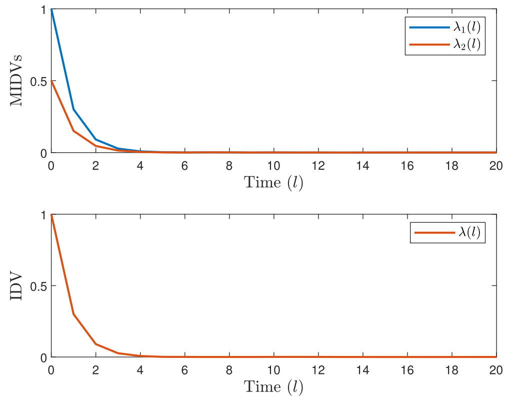

Fig. 7. The trajectories of IDV in [35] and MIDVs in this article.

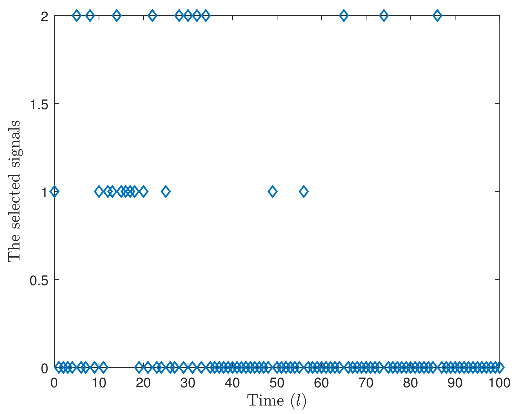

Fig. 8. The selected signals under MVET-SC protocol.

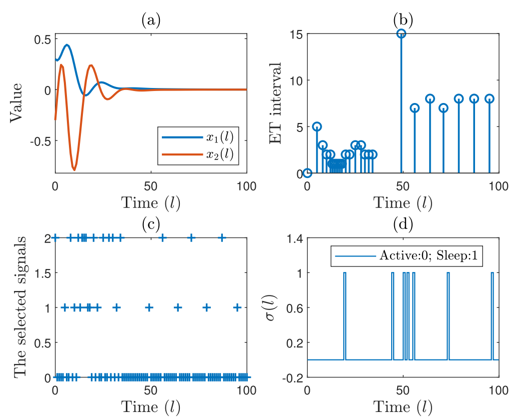

Fig. 9. (a) System states. (b) The release instants of MVETS. (c) The selected signals. (d) Response of RADoS attacks. (Case 1).

than a single IDV and the convergence speed is almost same between them. In general, the design flexibility and dynamicity can be improved by utilizing MVETS. Meanwhile, the overall performance of MVETS is not inferior to DETS.

From the perspective of scheduling, the transmitted signals selected by MVET-SC protocol are displayed in Fig. 8. We denote the numbers 1 and 2 as the selected sensor nodes. In particular, the number 0 represents that the MVETS condition is not met and no sensor node will be scheduled. It is worth mentioning that one of the elements of the measured output can be transferred through a communication channel if

TABLE II
DIFFERENT CASES OF PROBABILITIES

Case 1	$\zeta_{11} = 0.15,\ \zeta_{12} = 0.85,\ \zeta_{21} = 0.75,$ $\zeta_{22} = 0.25,\ \bar{\sigma} = 0.04.$
Case 2	$\zeta_{11} = 0.4,\ \zeta_{12} = 0.6,\ \zeta_{21} = 0.55,$ $\zeta_{22} = 0.45,\ \bar{\sigma} = 0.16.$
Case 3	$\zeta_{11} = 0.65,\ \zeta_{12} = 0.35,\ \zeta_{21} = 0.15,$ $\zeta_{22} = 0.85,\ \bar{\sigma} = 0.28.$

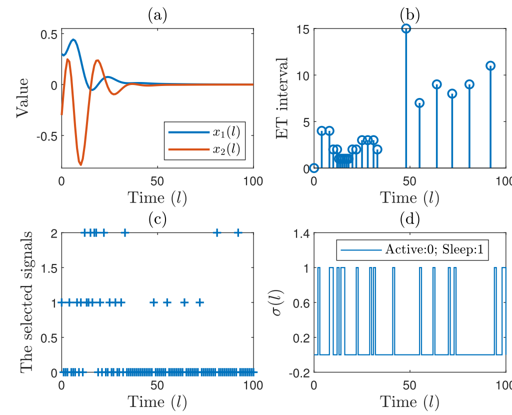

Fig. 10. (a) System states. (b) The release instants of MVETS. (c) The selected signals. (d) Response of RADoS attacks. (Case 2).

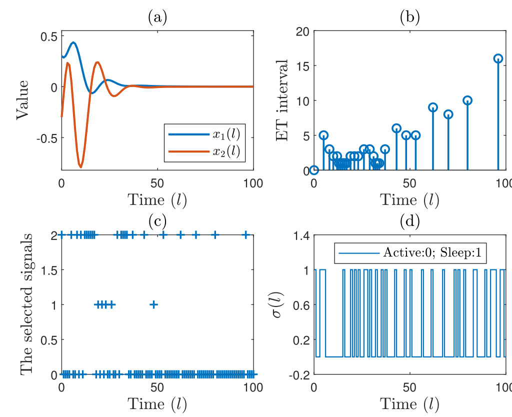

Fig. 11. (a) System states. (b) The release instants of MVETS. (c) The selected signals. (d) Response of RADoS attacks. (Case 3).

the MVETS condition holds. Obviously, it not only alleviates network occupation, but also effectively avoids the occurrence of data conflicts. On the whole, the validity of the theoretical results in this paper is once again illustrated.

In this article, the RADoS attacks and the proposed MVET-SC protocol are simultaneously considered. Hence, we further investigate the convergence of system states and the number of ET instants under different occurrence probabilities of RADoS attacks and transition probabilities. On the ground of other parameters in the aforementioned simulation example, the parameters of different cases are listed in TABLE II. Then, the corresponding simulation results are plotted in Figs. 9-11. It is apparently observed from these cases that the system states can converge the equilibrium point under the designed control strategy. Despite the different occurrence situations of RADoS attacks, the convergence times of system states in these cases are just a subtle difference. Besides, since the number of ET instants in these cases is just sightly change, the overall ET performance is not affected to a great extent. Therefore, the proposed control scheme is feasible and effective.

V. Conclusion

An OR observer-based secure control issue has been investigated for IT-2 fuzzy system subject to RADoS attacks. Under the consideration of malicious attack behavior, a compensation strategy is utilized to relieve the adverse effect brought by RADoS attacks. In an effort to lessen the network bandwidth pressure, a MVET-SC protocol is proposed to boost the design flexibility and decrease the occurrence of data congestion in the shared communication channel. Taking account of the abnormal measurement signal, the OR observer is constructed by applying a saturation function. Furthermore, we consider the fragility problem in the adopted control approach, which can appropriately tolerate the gain variations. By virtue of vector augmentation technique, an augmented fuzzy model is derived on the basis of the aforementioned factors. Then, a range of sufficient design criteria has been presented to assure the asymptotic stability of the constructed augmented system. The gain matrices of OR observer and non-fragile controller are obtained. Eventually, a MSDS example is conducted to prove the feasibility of the developed secure control scheme.

Appendix

The relevant parameters in Theorem 2 are listed as follows.

$$\bar{S}^{1T}_{hr} = \begin{bmatrix} R_h^T B_r^T Y^T & R_h^T (B_p^T - B_r^T) Y^T & 0_{2N+12} \end{bmatrix},$$
$$Q_h^1 = \begin{bmatrix} 0_{N+8} & N_h & 0_{N+5} \end{bmatrix},\ Q_h^2 = \sqrt{\tau_h} Q_h^1,\ \bar{S}^{2T}_{hr} = \bar{S}^{1T}_{hr},$$
$$\vec{\Psi}^1_{prht} = \begin{bmatrix} 2\vec{\mathcal{P}}_t & * \\ \vec{\Sigma}_{prht} + \vec{\Sigma}_{phrt} & \mathcal{U} \end{bmatrix},\ \mathcal{U} = \begin{bmatrix} \mathcal{U}_1 & \mathcal{U}_2 \\ \mathcal{U}_3 & \mathcal{U}_4 \\ \mathcal{U}_5 & \mathcal{U}_6 \end{bmatrix},$$
$$\vec{\Psi}^2_{prht} = \begin{bmatrix} 2\vec{\mathcal{P}}_t & * \\ \sqrt{\tau_h}\vec{\Sigma}_{prht} + \sqrt{\tau_r}\vec{\Sigma}_{phrt} & \mathcal{V} \end{bmatrix},\ \mathcal{V} = \begin{bmatrix} \mathcal{V}_1 & \mathcal{V}_2 \\ \mathcal{V}_3 & \mathcal{V}_4 \\ \mathcal{V}_5 & \mathcal{V}_6 \end{bmatrix},$$
$$\vec{\mathcal{P}}_t = \mathrm{diag}\{\bar{P}_{1,t} - sym\{Y\}, \bar{P}_{2,t} - sym\{Y\}, \bar{P}_{3,t} - sym\{Y\}, \bar{P}_{1,t} - sym\{Y\}, \bar{P}_{2,t} - sym\{Y\}, \bar{P}_{3,t} - sym\{Y\}, -I, \Theta - sym\{Y\}, \Theta - sym\{Y\}, -I_{N-1}\},$$
$$\vec{\Sigma}_{prht} = \begin{bmatrix} \tilde{\mathcal{F}}^T_{1prht} & \tilde{\mathcal{F}}^T_{2prht} & \tilde{C}^T_{2p} & \tilde{C}^{1T}_{1p} & \tilde{C}^{2T}_{1p} & 0_{N-1} \\ \tilde{\mathcal{F}}^T_{3prht} & \tilde{\mathcal{F}}^T_{4prht} & 0 & 0 & -\tilde{\varepsilon}^2_M Y^T & 0_{N-1} \\ \tilde{\mathcal{F}}^T_{5r} & 0 & 0 & 0 & 0 & 0_{N-1} \\ \tilde{B}^T_{wp} & 0 & 0 & 0 & 0 & 0_{N-1} \\ 0^T_N & 0^T_N & 0^T_N & 0^T_N & 0^T_N & 0^N_{N-1} \end{bmatrix},$$
$$\tilde{\mathcal{F}}^T_{1prht} = \begin{bmatrix} \tilde{\mathcal{F}}^1_{11} & \tilde{\mathcal{F}}^1_{12} & \bar{\sigma} C^T_{1p}\Phi^T_t Y^T \\ \bar{\sigma} C^T_{1p}\Phi^T_t \mathcal{H}^T_1 U_r & \tilde{\mathcal{F}}^1_{22} & \bar{\sigma} C^T_{1p}\Phi^T_t Y^T \\ \tilde{\mathcal{F}}^1_{31} & \tilde{\mathcal{F}}^1_{32} & \bar{\sigma}\Phi^T_t Y^T + \bar{\Phi}^T_t Y^T \end{bmatrix},$$
$$\tilde{\mathcal{F}}^T_{2prht} = \begin{bmatrix} \breve{\sigma}\tilde{\Pi}_{prt} & -\breve{\sigma}\tilde{\Pi}_{prt} & \breve{\sigma} C^T_{1p}\Phi^T_t Y^T \\ \breve{\sigma}\tilde{\Pi}_{prt} & -\breve{\sigma}\tilde{\Pi}_{prt} & \breve{\sigma} C^T_{1p}\Phi^T_t Y^T \\ -\breve{\sigma}\Phi^T_t\mathcal{H}^T_1 U_r & \breve{\sigma}\Phi^T_t\mathcal{H}^T_1 U_r & -\breve{\sigma}\Phi^T_t Y^T \end{bmatrix},$$
$$\tilde{\mathcal{F}}^T_{3prht} = \begin{bmatrix} -\bar{\sigma}\Phi^T_t\mathcal{H}^T_1 U_r & \bar{\sigma}\Phi^T_t\mathcal{H}^T_1 U_r & -\bar{\sigma}\Phi^T_t Y^T \end{bmatrix},$$
$$\tilde{\mathcal{F}}^T_{4prht} = \begin{bmatrix} -\breve{\sigma}\Phi^T_t\mathcal{H}^T_1 U_r & \breve{\sigma}\Phi^T_t\mathcal{H}^T_1 U_r & -\breve{\sigma}\Phi^T_t Y^T \end{bmatrix},$$
$$\tilde{\mathcal{F}}^T_{5r} = \begin{bmatrix} U_r & -U_r & 0 \end{bmatrix},\ \tilde{C}^1_{1p} = \begin{bmatrix} \tilde{\varepsilon}^1_M Y C_{1p} & \tilde{\varepsilon}^1_M Y C_{1p} & 0 \end{bmatrix},$$
$$\tilde{B}^T_{wp} = \begin{bmatrix} 0 & B^T_{wp} Y^T & 0 \end{bmatrix},\ \tilde{C}^2_{1p} = \begin{bmatrix} \tilde{\varepsilon}^2_M Y C_{1p} & \tilde{\varepsilon}^2_M Y C_{1p} & 0 \end{bmatrix},$$
$$\tilde{\mathcal{F}}^1_{11} = A^T_r Y^T + V_h B^T_r + \bar{\sigma} C^T_{1p}\Phi^T_t\mathcal{H}^T_1 U_r - C^T_{1r}\mathcal{H}^T_1 U_r,$$
$$\tilde{\mathcal{F}}^1_{12} = A^T_p Y^T - A^T_r Y^T + V_h B^T_p - V_h B^T_r - \bar{\sigma} C^T_{1p}\Phi^T_t\mathcal{H}^T_1 U_r + C^T_{1r}\mathcal{H}^T_1 U_r,\ \tilde{\varepsilon}^1_M = \sqrt{\bar{\kappa}\varepsilon^1_M},\ \tilde{\varepsilon}^2_M = \sqrt{\bar{\kappa}\varepsilon^2_M},$$
$$\tilde{\mathcal{F}}^1_{22} = A^T_p Y^T - \bar{\sigma} C^T_{1p}\Phi^T_t\mathcal{H}^T_1 U_r,\ \tilde{\Pi}_{prt} = C^T_{1p}\Phi^T_t\mathcal{H}^T_1 U_r,$$
$$\tilde{\mathcal{F}}^1_{31} = \bar{\sigma}\Phi^T_t\mathcal{H}^T_1 U_r + \bar{\Phi}^T_t\mathcal{H}^T_1 U_r,\ \tilde{\mathcal{F}}^1_{32} = -\tilde{\mathcal{F}}^1_{31},$$
$$\mathcal{U}_1 = \begin{bmatrix} \mathcal{U}^1_{11} & -2\Lambda_{12} & -2\Lambda_{13} & -2\Lambda_{14} \\ -2\Lambda_{21} & \mathcal{U}^1_{22} & -2\Lambda_{23} & -2\Lambda_{24} \\ -2\Lambda_{31} & -2\Lambda_{32} & \mathcal{U}^1_{33} & -2\Lambda_{34} \end{bmatrix},$$
$$\mathcal{U}_2 = \begin{bmatrix} \mathcal{U}^2_{11} & -2\Lambda_{16} & -2\Lambda_{17} & \cdots & -2\Lambda_{1\aleph} \\ \mathcal{U}^2_{21} & -2\Lambda_{26} & -2\Lambda_{27} & \cdots & -2\Lambda_{2\aleph} \\ \mathcal{U}^2_{31} & -2\Lambda_{36} & -2\Lambda_{37} & \cdots & -2\Lambda_{3\aleph} \end{bmatrix},$$
$$\mathcal{U}_3 = \begin{bmatrix} -2\Lambda_{41} & -2\Lambda_{42} & -2\Lambda_{43} & -2\bar{\kappa}\Theta - 2\Lambda_{44} \\ \mathcal{U}^3_{21} & \mathcal{U}^3_{22} & \mathcal{U}^3_{23} & \mathcal{U}^3_{24} \\ -2\Lambda_{61} & -2\Lambda_{62} & -2\Lambda_{63} & -2\Lambda_{64} \end{bmatrix},$$
$$\mathcal{U}_4 = \begin{bmatrix} \mathcal{U}^4_{11} & -2\Lambda_{46} & -2\Lambda_{47} & \cdots & -2\Lambda_{4\aleph} \\ \mathcal{U}^4_{21} & -2\Lambda_{56} & -2\Lambda_{57} & \cdots & -2\Lambda_{5\aleph} \\ -2\Lambda_{65} & \mathcal{U}^4_{32} & -2\Lambda_{67} & \cdots & -2\Lambda_{6\aleph} \end{bmatrix},$$
$$\mathcal{U}_5 = \begin{bmatrix} -2\Lambda_{71} & -2\Lambda_{72} & -2\Lambda_{73} & -2\Lambda_{74} \\ \vdots & \vdots & \vdots & \vdots \\ -2\Lambda_{\aleph 1} & -2\Lambda_{\aleph 2} & -2\Lambda_{\aleph 3} & -2\Lambda_{\aleph 4} \end{bmatrix},$$
$$\mathcal{U}_6 = \begin{bmatrix} -2\Lambda_{75} & -2\Lambda_{76} & \mathcal{U}^6_{13} & -2\Lambda_{7\aleph} & \\ \vdots & \vdots & \vdots & \vdots & \\ & -2\Lambda_{\aleph 5} & -2\Lambda_{\aleph 6} & -2\Lambda_{\aleph 7} & \mathcal{U}^6_{34} \end{bmatrix},$$
$$\mathcal{U}^1_{11} = -2P_{1,t} - 2\Lambda_{11},\ \mathcal{U}^1_{22} = -2P_{2,t} - 2\Lambda_{22},$$
$$\mathcal{U}^1_{33} = -2P_{3,t} - 2\Lambda_{33},\ \aleph = N+6,$$
$$\mathcal{U}^2_{11} = 2\bar{\sigma}\rho_2 C^T_{1p}\Phi^T_t\mathcal{H}^T - \rho_2 C^T_{1r}\mathcal{H}^T - \rho_2 C^T_{1h}\mathcal{H}^T - 2\Lambda_{15},$$
$$\mathcal{U}^2_{21} = 2\bar{\sigma}\rho_2 C^T_{1p}\Phi^T_t\mathcal{H}^T - 2\Lambda_{25},$$
$$\mathcal{U}^4_{11} = -2\bar{\sigma}\rho_2\Phi^T_t\mathcal{H}^T - 2\Lambda_{45},$$
$$\mathcal{U}^2_{31} = 2\bar{\sigma}\rho_2\Phi^T_t\mathcal{H}^T + 2\rho_2\bar{\Phi}^T_t\mathcal{H}^T - 2\Lambda_{35},$$
$$\mathcal{U}^3_{21} = 2\bar{\sigma}\rho_2\mathcal{H}\Phi_t C_{1p} - \rho_2\mathcal{H}C_{1r} - \rho_2\mathcal{H}C_{1h} - 2\Lambda_{51},$$
$$\mathcal{U}^3_{22} = 2\bar{\sigma}\rho_2\mathcal{H}\Phi_t C_{1p} - 2\Lambda_{52},\ \mathcal{U}^4_{21} = -2\rho_2 I - 2\Lambda_{55},$$
$$\mathcal{U}^3_{23} = 2\bar{\sigma}\rho_2\mathcal{H}\Phi_t + 2\rho_2\mathcal{H}\bar{\Phi}_t - 2\Lambda_{53},$$
$$\mathcal{U}^3_{24} = -2\bar{\sigma}\rho_2\mathcal{H}\Phi_t - 2\Lambda_{54},\ \mathcal{U}^4_{32} = -2\gamma^2 I - 2\Lambda_{66},$$
$$\mathcal{U}^6_{13} = 2\frac{\theta_1}{a_1}(\kappa_1 + \rho_1 - 1)I - 2\Lambda_{77},$$
$$\mathcal{U}^6_{34} = 2\frac{\theta_N}{a_N}(\kappa_N + \rho_1 - 1)I - 2\Lambda_{\aleph\aleph},$$
$$\mathcal{V}_1 = \begin{bmatrix} \mathcal{V}^1_{11} & \bar{\tau}_{hr}\Lambda_{12} & \bar{\tau}_{hr}\Lambda_{13} & \bar{\tau}_{hr}\Lambda_{14} \\ \bar{\tau}_{hr}\Lambda_{21} & \mathcal{V}^1_{22} & \bar{\tau}_{hr}\Lambda_{23} & \bar{\tau}_{hr}\Lambda_{24} \\ \bar{\tau}_{hr}\Lambda_{31} & \bar{\tau}_{hr}\Lambda_{32} & \mathcal{V}^1_{33} & \bar{\tau}_{hr}\Lambda_{34} \end{bmatrix},$$
$$\mathcal{V}_2 = \begin{bmatrix} \mathcal{V}^2_{11} & \bar{\tau}_{hr}\Lambda_{16} & \bar{\tau}_{hr}\Lambda_{17} & \cdots & \bar{\tau}_{hr}\Lambda_{1\aleph} \\ \mathcal{V}^2_{21} & \bar{\tau}_{hr}\Lambda_{26} & \bar{\tau}_{hr}\Lambda_{27} & \cdots & \bar{\tau}_{hr}\Lambda_{2\aleph} \\ \mathcal{V}^2_{31} & \bar{\tau}_{hr}\Lambda_{36} & \bar{\tau}_{hr}\Lambda_{37} & \cdots & \bar{\tau}_{hr}\Lambda_{3\aleph} \end{bmatrix},$$
$$\mathcal{V}_3 = \begin{bmatrix} \bar{\tau}_{hr}\Lambda_{41} & \bar{\tau}_{hr}\Lambda_{42} & \bar{\tau}_{hr}\Lambda_{43} & \mathcal{V}^3_{14} \\ \mathcal{V}^3_{21} & \mathcal{V}^3_{22} & \mathcal{V}^3_{23} & \mathcal{V}^3_{24} \\ \bar{\tau}_{hr}\Lambda_{61} & \bar{\tau}_{hr}\Lambda_{62} & \bar{\tau}_{hr}\Lambda_{63} & \bar{\tau}_{hr}\Lambda_{64} \end{bmatrix},$$

$$\mathcal{V}_5 = -\frac{1}{2}\bar{\tau}_{hr}\mathcal{U}_5,$$

$$\mathcal{V}_4 = \begin{bmatrix} \mathcal{V}_{11}^4 & \bar{\tau}_{hr}\Lambda_{46} & \bar{\tau}_{hr}\Lambda_{47} & \cdots & \bar{\tau}_{hr}\Lambda_{4\aleph} \\ \mathcal{V}_{21}^4 & \bar{\tau}_{hr}\Lambda_{56} & \bar{\tau}_{hr}\Lambda_{57} & \cdots & \bar{\tau}_{hr}\Lambda_{5\aleph} \\ \bar{\tau}_{hr}\Lambda_{65} & \mathcal{V}_{32}^4 & \bar{\tau}_{hr}\Lambda_{67} & \cdots & \bar{\tau}_{hr}\Lambda_{6\aleph} \end{bmatrix},$$

$$\mathcal{V}_6 = \begin{bmatrix} \bar{\tau}_{hr}\Lambda_{75} & \bar{\tau}_{hr}\Lambda_{76} & \mathcal{V}_{13}^6 & \bar{\tau}_{hr}\Lambda_{7\aleph} \\ \vdots & \vdots & \vdots & \vdots \\ \bar{\tau}_{hr}\Lambda_{\aleph 5} & \bar{\tau}_{hr}\Lambda_{\aleph 6} & \bar{\tau}_{hr}\Lambda_{\aleph 7} & \mathcal{V}_{24}^6 \end{bmatrix},$$

$$\mathcal{V}_{11}^1 = -\tau_{hr}P_{1,t} + \bar{\tau}_{hr}\Lambda_{11},\ \mathcal{V}_{22}^1 = -\tau_{hr}P_{2,t} + \bar{\tau}_{hr}\Lambda_{22},$$

$$\mathcal{V}_{33}^1 = -\tau_{hr}P_{3,t} + \bar{\tau}_{hr}\Lambda_{33},\ \tau_{hr} = \tau_h + \tau_r,\ \bar{\tau}_{hr} = 2 - \tau_{hr},$$

$$\mathcal{V}_{11}^2 = \rho_2(\tau_{hr}\bar{\sigma}C_{1p}^T\Phi_t^T\mathcal{H}^T - \tau_h C_{1r}^T\mathcal{H}^T - \tau_r C_{1h}^T\mathcal{H}^T) + \bar{\tau}_{hr}\Lambda_{15},$$

$$\mathcal{V}_{21}^2 = \tau_{hr}\bar{\sigma}\rho_2 C_{1p}^T\Phi_t^T\mathcal{H}^T + \bar{\tau}_{hr}\Lambda_{25},$$

$$\mathcal{V}_{31}^2 = \tau_{hr}\vec{\sigma}\rho_2\Phi_t^T\mathcal{H}^T + \tau_{hr}\rho_2\bar{\Phi}_t^T\mathcal{H}^T + \bar{\tau}_{hr}\Lambda_{35},$$

$$\mathcal{V}_{21}^3 = \tau_{hr}\bar{\sigma}\rho_2\mathcal{H}\Phi_t C_{1p} - \tau_h\rho_2\mathcal{H}C_{1r} - \tau_r\rho_2\mathcal{H}C_{1h} + \bar{\tau}_{hr}\Lambda_{51},$$

$$\mathcal{V}_{22}^3 = \tau_{hr}\bar{\sigma}\rho_2\mathcal{H}\Phi_t C_{1p} + \bar{\tau}_{hr}\Lambda_{52},$$

$$\mathcal{V}_{23}^3 = \tau_{hr}\vec{\sigma}\rho_2\mathcal{H}\Phi_t + \tau_{hr}\rho_2\mathcal{H}\bar{\Phi}_t + \bar{\tau}_{hr}\Lambda_{53},$$

$$\mathcal{V}_{24}^3 = -\tau_{hr}\bar{\sigma}\rho_2\mathcal{H}\Phi_t + \bar{\tau}_{hr}\Lambda_{54},\ \mathcal{V}_{14}^3 = -\tau_{hr}\bar{\kappa}\Theta + \bar{\tau}_{hr}\Lambda_{44},$$

$$\mathcal{V}_{11}^4 = -\tau_{hr}\rho_2\bar{\sigma}\Phi_t^T\mathcal{H}^T + \bar{\tau}_{hr}\Lambda_{45},$$

$$\mathcal{V}_{21}^4 = -\tau_{hr}\rho_2 I + \bar{\tau}_{hr}\Lambda_{55},\ \mathcal{V}_{32}^4 = -\tau_{hr}\gamma^2 I + \bar{\tau}_{hr}\Lambda_{66},$$

$$\mathcal{V}_{13}^6 = \tau_{hr}\frac{\theta_1}{a_1}(\kappa_1 + \rho_1 - 1)I + \bar{\tau}_{hr}\Lambda_{77},$$

$$\mathcal{V}_{24}^6 = \tau_{hr}\frac{\theta_N}{a_N}(\kappa_N + \rho_1 - 1)I + \bar{\tau}_{hr}\Lambda_{\aleph\aleph}.$$

REFERENCES

[1] S. Hu, X. Ge, Y. Li, X. Chen, X. Xie, and D. Yue, "Resilient load frequency control of multi-area power systems under DoS attacks," *IEEE Trans. Inf. Forensics Security*, vol. 18, pp. 936–947, 2023.

[2] K.-D. Lu, G.-Q. Zeng, X. Luo, J. Weng, Y. Zhang, and M. Li, "An adaptive resilient load frequency controller for smart grids with DoS attacks," *IEEE Trans. Veh. Technol.*, vol. 69, no. 5, pp. 4689–4699, May 2020.

[3] S. S. Xu, H.-C. Huang, Y.-C. Kung, and Y.-Y. Chu, "A networked multirobot CPS with artificial immune fuzzy optimization for distributed formation control of embedded mobile robots," *IEEE Trans. Ind. Informat.*, vol. 16, no. 1, pp. 414–422, Jan. 2020.

[4] L. Zha, R. Liao, J. Liu, X. Xie, E. Tian, and J. Cao, "Dynamic event-triggered output feedback control for networked systems subject to multiple cyber attacks," *IEEE Trans. Cybern.*, vol. 52, no. 12, pp. 13800–13808, Dec. 2022.

[5] J. Yang, Q. Zhong, K. Shi, and S. Zhong, "Co-design of observer-based fault detection filter and dynamic event-triggered controller for wind power system under dual alterable DoS attacks," *IEEE Trans. Inf. Forensics Security*, vol. 17, pp. 1270–1284, 2022.

[6] B.-F. Yue, M.-Y. Su, X.-Z. Jin, and W.-W. Che, "Event-triggered MFAC of nonlinear NCSs against sensor faults and DoS attacks," *IEEE Trans. Circuits Syst. II, Exp. Briefs*, vol. 69, no. 11, pp. 4409–4413, Nov. 2022.

[7] J. Liu, E. Gong, L. Zha, E. Tian, and X. Xie, "Observer-based security fuzzy control for nonlinear networked systems under weighted try-once-discard protocol," *IEEE Trans. Fuzzy Syst.*, vol. 31, no. 11, pp. 3853–3865, Apr. 2023.

[8] E. Tian, H. Chen, C. Wang, and L. Wang, "Security-ensured state of charge estimation of lithium-ion batteries subject to malicious attacks," *IEEE Trans. Smart Grid*, vol. 14, no. 3, pp. 2250–2261, May 2023.

[9] Z. Gu, T. Yin, and Z. Ding, "Path tracking control of autonomous vehicles subject to deception attacks via a learning-based event-triggered mechanism," *IEEE Trans. Neural Netw. Learn. Syst.*, vol. 32, no. 12, pp. 5644–5653, Dec. 2021.

[10] S. Hu, D. Yue, C. Dou, X. Xie, Y. Ma, and L. Ding, "Attack-resilient event-triggered fuzzy interval type-2 filter design for networked nonlinear systems under sporadic denial-of-service jamming attacks," *IEEE Trans. Fuzzy Syst.*, vol. 30, no. 1, pp. 190–204, Jan. 2022.

[11] C. Wu, L. Wu, J. Liu, and Z.-P. Jiang, "Active defense-based resilient sliding mode control under denial-of-service attacks," *IEEE Trans. Inf. Forensics Security*, vol. 15, pp. 237–249, 2020.

[12] J. Liu, Y. Dong, L. Zha, E. Tian, and X. Xie, "Event-based security tracking control for networked control systems against stochastic cyber-attacks," *Inf. Sci.*, vol. 612, pp. 306–321, Oct. 2022.

[13] K. Zhang, B. Zhou, W. X. Zheng, and G.-R. Duan, "Event-triggered and self-triggered gain scheduled control of linear systems with input constraints," *IEEE Trans. Syst., Man, Cybern., Syst.*, vol. 52, no. 10, pp. 6452–6463, Oct. 2022.

[14] I. Ahmad, X. Ge, and Q.-L. Han, "Decentralized dynamic event-triggered communication and active suspension control of in-wheel motor driven electric vehicles with dynamic damping," *IEEE/CAA J. Autom. Sinica*, vol. 8, no. 5, pp. 971–986, May 2021.

[15] Y. Pan and G.-H. Yang, "Event-triggered fuzzy control for nonlinear networked control systems," *Fuzzy Sets Syst.*, vol. 329, pp. 91–107, Dec. 2017.

[16] E. Tian and C. Peng, "Memory-based event-triggering H_∞ load frequency control for power systems under deception attacks," *IEEE Trans. Cybern.*, vol. 50, no. 11, pp. 4610–4618, Nov. 2020.

[17] J. Liu, Z.-G. Wu, D. Yue, and J. H. Park, "Stabilization of networked control systems with hybrid-driven mechanism and probabilistic cyber attacks," *IEEE Trans. Syst., Man, Cybern., Syst.*, vol. 51, no. 2, pp. 943–953, Feb. 2021.

[18] C. Wu, X. Zhao, B. Wang, W. Xing, L. Liu, and X. Wang, "Model-based dynamic event-triggered control for cyber-physical systems subject to dynamic quantization and DoS attacks," *IEEE Trans. Netw. Sci. Eng.*, vol. 9, no. 4, pp. 2406–2417, Jul. 2022.

[19] W. Gai, S. Li, J. Zhang, Y. Zheng, and M. Zhong, "Dynamic event-triggered H_i/H_∞ optimization approach to fault detection for unmanned aerial vehicles," *IEEE Trans. Instrum. Meas.*, vol. 71, pp. 1–11, 2022.

[20] Z. Su, S. Ding, L. Wang, and X. Xie, "Stabilization of memristor-based Chua's circuits via dynamic event-triggered mechanism," *IEEE Trans. Circuits Syst. II, Exp. Briefs*, vol. 69, no. 9, pp. 3809–3813, Sep. 2022.

[21] Y. Tan, Y. Yuan, X. Xie, E. Tian, and J. Liu, "Observer-based event-triggered control for interval type-2 fuzzy networked system with network attacks," *IEEE Trans. Fuzzy Syst.*, vol. 31, no. 8, pp. 2788–2798, Aug. 2023.

[22] J. Cheng, H. Yan, J. H. Park, and G. Zong, "Output-feedback control for fuzzy singularly perturbed systems: A nonhomogeneous stochastic communication protocol approach," *IEEE Trans. Cybern.*, vol. 53, no. 1, pp. 76–87, Jan. 2023.

[23] Y. Dong, Y. Song, and G. Wei, "Efficient model-predictive control for networked interval type-2 T–S fuzzy system with stochastic communication protocol," *IEEE Trans. Fuzzy Syst.*, vol. 29, no. 2, pp. 286–297, Feb. 2021.

[24] D. Liu, Z. Wang, Y. Liu, F. E. Alsaadi, and F. E. Alsaadi, "Recursive state estimation for stochastic complex networks under round-robin communication protocol: Handling packet disorders," *IEEE Trans. Netw. Sci. Eng.*, vol. 8, no. 3, pp. 2455–2468, Jul. 2021.

[25] X. Wan, Z. Wang, M. Wu, and X. Liu, "State estimation for discrete time-delayed genetic regulatory networks with stochastic noises under the round-robin protocols," *IEEE Trans. Nanobiosci.*, vol. 17, no. 2, pp. 145–154, Apr. 2018.

[26] J. Cheng, J. H. Park, and Z.-G. Wu, "Observer-based asynchronous control of nonlinear systems with dynamic event-based try-once-discard protocol," *IEEE Trans. Cybern.*, vol. 52, no. 12, pp. 12638–12648, Dec. 2022.

[27] Y. Ju, G. Wei, D. Ding, and S. Liu, "A novel fault detection method under weighted try-once-discard scheduling over sensor networks," *IEEE Trans. Control Netw. Syst.*, vol. 7, no. 3, pp. 1489–1499, Sep. 2020.

[28] W. Chen, J. Hu, X. Yu, D. Chen, and Z. Wu, "Robust fault detection for uncertain delayed systems with measurement outliers under stochastic communication protocol," *IEEE Trans. Signal Inf. Process. over Netw.*, vol. 8, pp. 684–701, 2022.

[29] X. Wan, Z. Wang, Q.-L. Han, and M. Wu, "A recursive approach to quantized H_∞ state estimation for genetic regulatory networks under stochastic communication protocols," *IEEE Trans. Neural Netw. Learn. Syst.*, vol. 30, no. 9, pp. 2840–2852, Sep. 2019.

[30] X.-X. Ren, G.-H. Yang, and X.-G. Zhang, "Statistical-based optimal ϵ-stealthy attack under stochastic communication protocol: An application to networked permanent magnet synchronous machine systems," *IEEE Trans. Ind. Electron.*, vol. 70, no. 1, pp. 1036–1046, Jan. 2023.

[31] J. Li, Z. Wang, H. Dong, and X. Yi, "Outlier-resistant observer-based control for a class of networked systems under encoding–decoding mechanism," *IEEE Syst. J.*, vol. 16, no. 1, pp. 922–932, Mar. 2022.

[32] Z. Zhang and J. Dong, "Observer-based interval type-2 H_2–L_∞/H_∞ mixed fuzzy control for uncertain nonlinear systems under measurement outliers," *IEEE Trans. Syst., Man, Cybern., Syst.*, vol. 51, no. 12, pp. 7652–7662, Dec. 2021.

[33] L. Zou, Z. Wang, H. Geng, and X. Liu, "Set-membership filtering subject to impulsive measurement outliers: A recursive algorithm," *IEEE/CAA J. Autom. Sinica*, vol. 8, no. 2, pp. 377–388, Feb. 2021.

[34] J. Li, Z. Wang, H. Dong, and G. Ghinea, "Outlier-resistant remote state estimation for recurrent neural networks with mixed time-delays," *IEEE Trans. Neural Netw. Learn. Syst.*, vol. 32, no. 5, pp. 2266–2273, May 2021.

[35] J. Cheng, J. H. Park, H. Yan, and Z.-G. Wu, "An event-triggered round-robin protocol to dynamic output feedback control for nonhomogeneous Markov switching systems," *Automatica*, vol. 145, Nov. 2022, Art. no. 110525.

[36] Y. Yang, Y. Niu, and H.-K. Lam, "Sliding-mode control for interval type-2 fuzzy systems: Event-triggering WTOD scheme," *IEEE Trans. Cybern.*, vol. 53, no. 6, pp. 3771–3781, Sep. 2023.

[37] Z. Zhang, Y. Niu, Z. Cao, and J. Song, "Security sliding mode control of interval type-2 fuzzy systems subject to cyber attacks: The stochastic communication protocol case," *IEEE Trans. Fuzzy Syst.*, vol. 29, no. 2, pp. 240–251, Feb. 2021.

[38] X. Zheng, H. Zhang, Z. Wang, C. Zhang, and H. Yan, "Finite-time dynamic event-triggered distributed H_∞ filtering for T–S fuzzy systems," *IEEE Trans. Fuzzy Syst.*, vol. 30, no. 7, pp. 2476–2486, Jul. 2022.

[39] C. Peng, M. Wu, X. Xie, and Y.-L. Wang, "Event-triggered predictive control for networked nonlinear systems with imperfect premise matching," *IEEE Trans. Fuzzy Syst.*, vol. 26, no. 5, pp. 2797–2806, Oct. 2018.

[40] X. Bu, H. Dong, Z. Wang, and H. Liu, "Non-fragile distributed fault estimation for a class of nonlinear time-varying systems over sensor networks: The finite-horizon case," *IEEE Trans. Signal Inf. Process. over Netw.*, vol. 5, no. 1, pp. 61–69, Mar. 2019.

[41] X. Li and D. Ye, "Asynchronous event-triggered control for networked interval type-2 fuzzy systems against DoS attacks," *IEEE Trans. Fuzzy Syst.*, vol. 29, no. 2, pp. 262–274, Feb. 2021.

[42] H. Li, C. Wu, S. Yin, and H.-K. Lam, "Observer-based fuzzy control for nonlinear networked systems under unmeasurable premise variables," *IEEE Trans. Fuzzy Syst.*, vol. 24, no. 5, pp. 1233–1245, Oct. 2016.

[43] C. Peng, S. Ma, and X. Xie, "Observer-based non-PDC control for networked T–S fuzzy systems with an event-triggered communication," *IEEE Trans. Cybern.*, vol. 47, no. 8, pp. 2279–2287, Aug. 2017.

[44] K. Tanaka and H. O. Wang, *Fuzzy Control Systems Design and Analysis: A Linear Matrix Inequality Approach*. New York, NY, USA: Wiley, 2001.

Jian Liu (Member, IEEE) received the Ph.D. degree in signal and information processing from the College of Communication and Information Engineering, Nanjing University of Posts and Telecommunications, Nanjing, China, in 2018. He is currently an Associate Professor with the College of Information Engineering, Nanjing University of Finance and Economics, Nanjing. He has published more than 40 articles in refereed international journals. His research interests include cyber-physical systems, networked control systems, complex dynamical networks, intelligent optimization algorithms, and network security. He received the Reward of Outstanding Reviewer for many international journals, such as *Computer Networks* and *Journal of Computational Science*. He has been serving as the Guest Editor for the special issue Fuzzy Modeling and Fuzzy Control Systems in Mathematics, since August 2022.

Jiachen Ke received the B.Ed. degree in science education from the School of Science, Huzhou University, Huzhou, China, in 2022. He is currently pursuing the M.S. degree in computer science and technology with the College of Information Engineering, Nanjing University of Finance and Economics, Nanjing, China. His research interests include fuzzy control, learning-based optimal control methods, and networked control systems.

Jinliang Liu (Member, IEEE) received the Ph.D. degree in control theory and control engineering from the School of Information Science and Technology, Donghua University, Shanghai, China, in 2011. He was a Post-Doctoral Research Associate with the School of Automation, Southeast University, Nanjing, China, from 2013 to 2016. He was a Visiting Researcher/a Visiting Scholar with the Department of Mechanical Engineering, The University of Hong Kong, Hong Kong, from 2016 to 2017. He was a Visiting Scholar with the Department of Electrical Engineering, Yeungnam University, Gyeongsan, South Korea, from 2017 to 2018. He is currently a Professor with the School of Computer Science, Nanjing University of Information Science and Technology, Jiangsu, China. His research interests include networked control systems, complex dynamical networks, and time-delay systems.

Xiangpeng Xie (Senior Member, IEEE) received the B.S. and Ph.D. degrees in engineering from Northeastern University, Shenyang, China, in 2004 and 2010, respectively. From 2010 to 2014, he was a Senior Engineer with Metallurgical Corporation of China Ltd., Beijing, China. He is currently a Professor with the Institute of Advanced Technology, Nanjing University of Posts and Telecommunications, Nanjing, China. His research interests include fuzzy modeling and control synthesis, state estimations, optimization in process industries, and intelligent optimization algorithms.

He serves as an Associate Editor for IEEE TRANSACTIONS ON FUZZY SYSTEMS, IEEE TRANSACTIONS ON INDUSTRIAL INFORMATICS, *International Journal of Fuzzy Systems*, and *International Journal of Control, Automation, and Systems*.

Engang Tian (Member, IEEE) received the B.S. degree in mathematics from Shandong Normal University, Jinan, China, in 2002, the M.Sc. degree in operations research and cybernetics from Nanjing Normal University, Nanjing, China, in 2005, and the Ph.D. degree in control theory and control engineering from Donghua University, Shanghai, China, in 2008.

From 2011 to 2012, he was a Post-Doctoral Research Fellow with The Hong Kong Polytechnic University, Hong Kong. From 2015 to 2016, he was a Visiting Scholar with the Department of Information Systems and Computing, Brunel University London, Uxbridge, U.K. From 2008 to 2018, he was an Associate Professor and then a Professor with the School of Electrical and Automation Engineering, Nanjing Normal University. In 2018, he was appointed as an Eastern Scholar by the Municipal Commission of Education, Shanghai. He joined the University of Shanghai for Science and Technology, Shanghai, where he is currently a Professor with the School of Optical-Electrical and Computer Engineering. He has published more than 100 articles in refereed international journals. His research interests include networked control systems, cyber attack, and nonlinear stochastic control and filtering.